

Assimilation of sea surface salinities from SMOS in an Arctic coupled ocean and sea ice reanalysis

Jiping Xie¹, Roshin P. Raj¹, Laurent Bertino¹, Justino Martínez², Carolina Gabarró^{2,3}, and Rafael Catany⁴

¹ Nansen Environmental and Remote Sensing Center and Bjerknes Centre for Climate Research, Bergen, Norway

² Institute of Marine Sciences, ICM-CSIC, Barcelona, Spain

³ Barcelona Expert Center, Barcelona, Spain

⁴ ARGANS, Plymouth, UK

Corresponding author: Jiping Xie, jiping.xie@nersc.no

Abstract

In the Arctic, the sea surface salinity (SSS) plays a key role in processes related to water mixing and sea ice. However, the lack of salinity observations causes large uncertainties in Arctic Ocean forecasts and reanalysis. Recently the Soil Moisture and Ocean Salinity (SMOS) satellite mission was used by the Barcelona Expert Centre to [develop](#) an Arctic SSS product. In this study, we evaluate the impact of assimilating this data in a coupled ocean-ice data assimilation system. Using the [Deterministic](#) Ensemble Kalman filter from July to December 2016, two assimilation runs [respectively](#) assimilated two successive versions of the SMOS SSS product, on top of a pre-existing reanalysis run. The runs were validated against independent [in-situ](#) salinity profiles in the Arctic. The results show that the biases and the Root Mean Squared Differences (RMSD) of SSS are reduced by 10% to 50% depending on areas, and [highlight](#) the [importance of assimilating satellite salinity data](#). The time series of Freshwater Content (FWC) further [shows](#) that its seasonal cycle can be adjusted by assimilation of the SSS products, which is encouraging for its use in a long-time reanalysis to [better reproduce](#) the Arctic water cycle.

Keywords: Arctic Ocean; Sea Surface Salinity; FWC; SMOS;

Style Definition: Normal: Font: (Asian) SimSun

Style Definition: Heading 1: Font: (Default) Calibri, (Asian) Calibri, (Asian) Chinese (China), (Other) , Snap to grid, Indent: Left: 0 cm, Hanging: 1.27 cm, No bullets or numbering

Style Definition: Heading 2: Font: (Default) Calibri, (Asian) Calibri, (Asian) Chinese (China), (Other) , Snap to grid, Indent: Left: 0 cm, Hanging: 1.27 cm, No bullets or numbering, Tab stops: 1.25 cm, Left

Style Definition: Heading 3: Font: (Default) Calibri, (Asian) Calibri, (Asian) Chinese (China), (Other) , Snap to grid, Indent: Left: 0 cm, Hanging: 1.27 cm, No bullets or numbering, Border: Bottom: (No border)

Style Definition: Heading 4: Font: (Default) Calibri, (Asian) Calibri, Font colour: Black, (Asian) Chinese (China), (Other) , Snap to grid, Indent: Left: 0 cm, Hanging: 1.27 cm, No bullets or numbering, Border: Bottom: (No border)

Style Definition: Heading 5,h5,Title 5,H5,OT Hdg 5,OT Hdg 51,.T5,h51,H51,h52,H52,h53,H53,h54,H54,h55,H55,sub-bullet,5 sub-bullet,Überschrift 51,Überschrift 511,Überschrift 512,Überschrift 513,Überschrift 514,Überschrift 515,H511,h511,Überschrift 5111,H521,h521,H531,h56: Font: (Default) Calibri, (Asian) Calibri, Font colour: Black, (Asian) Chinese (China), (Other) , Snap to grid, Indent: Left: 0 cm, Hanging: 1.27 cm, No bullets or numbering, Border: Bottom: (No border)

Style Definition: Heading 6,Title 6,h6,H6,H61,H62,H63,H64,H65,sub-dash,sd,5,Überschrift 61,Überschrift 611,Überschrift 612,Überschrift 613,Überschrift 614,Überschrift 615,Überschrift 6111,Überschrift 6121,Überschrift 6131,Überschrift 6141,Überschrift 616,Überschrift 6112: Font: (Default) Calibri, (Asian) Calibri, Font colour: Black, (Asian) Chinese (China), (Other) , Snap to grid, Indent: Left: 0 cm, Hanging: 1.27 cm, No bullets or numbering, Border: Bottom: (No border)

Style Definition: Heading 7: No bullets or numbering

Style Definition: Heading 8: No bullets or numbering

Style Definition: Heading 9: No bullets or numbering

Style Definition: Title

Style Definition: Normal (Web)

Style Definition: views-row

Style Definition: Comment Text

Style Definition: Footer

Style Definition: Header

Deleted: propose

Deleted: ¶

Formatted: Font: (Asian) SimSun, Font colour: Black

Deleted:

Deleted: put

Deleted: latest product to its advantage.

Deleted: show

Deleted: monitor

Formatted: Font: (Asian) SimSun, Font colour: Auto

25 **1. Introduction**

26 The Arctic Ocean is undergoing a dramatic warming, [resulting in the loss of sea ice](#)
27 [documented by previous studies](#) (Johannessen et al., 1999; Stroeve and Notz, 2018). [Sea](#)
28 ice melt contributes freshwater to the Arctic Ocean, together with other sources, and has far-
29 reaching effects on the Arctic Ocean environment (Carmack et al., 2016). The Arctic
30 observing system, [compared](#) to other oceans, lacks the capability to provide a complete
31 picture of ocean salinity, particularly because of obstruction by sea ice. A complete
32 reconstruction of Arctic environmental variables [thus](#) requires a data assimilative numerical
33 model capable of propagating information below sea ice during the winter as practiced by
34 ocean operational forecast systems (Dombrowsky, 2009; Fujii et al., 2019). As [with](#) other
35 ocean data assimilation (DA) applications, Arctic reanalysis products of ocean and sea ice
36 play an important role in understanding climate change and its mechanisms. In recent years,
37 many studies (Storto et al., 2019; Uotila et al., 2019) evaluated the quality of the Arctic
38 reanalysis products and recommended experiments [to maximize](#) the usefulness of new
39 [observations, as done in Kaminski et al. \(2015\) and Xie et al. \(2018\)](#). However, there are no
40 impact studies of salinity observations in the Arctic to our knowledge.
41 Ocean salinity has been used to study the water cycle for the last 20 years (e.g., Curry et al.,
42 2003; Boyer et al., 2005; Yu, 2011; Yu et al., 2017). [A recent review paper showed a](#)
43 [stabilization of the Freshwater Content \(FWC\) in the Arctic Basin, although observations](#)
44 [indicate that the Beaufort Gyre keeps getting fresher \(Solomon et al., 2021\)](#). [Salinity](#)
45 variations have far-reaching implications for ocean mixing, water mass formation, and ocean
46 general circulation, but [suffer from large uncertainties in the Arctic](#), mainly due to sparse
47 observations and the lack of a steady-state reference time period (e.g., Stroh et al., 2015; Xie
48 et al., 2019). Measuring sea surface salinity (SSS) from passive microwave remote sensing
49 is a comparatively new but promising way to reduce the uncertainty in salinity. Launched in
50 November 2009, the Microwave Imaging Radiometer using Aperture Synthesis (MIRAS)
51 instrument of the European Space Agency's (ESA) Soil Moisture and Ocean Salinity (SMOS)
52 mission measures the brightness temperature (T_B) on the sea surface. The passive 2-D
53 interferometric radiometer on the satellite operating in L-band (1.4 GHz) is sensitive to water
54 salinity and sufficiently free from electromagnetic interference (e.g., Font et al., 2010; Kerr et
55 al., 2010). Since May 2010, SMOS operationally provides SSS records over the global ocean
56 (Mecklenburg et al., 2012). [During the last 12 years, large improvements have been](#)
57 [introduced in the SMOS data processing chain, increasing the accuracy and coverage of the](#)
58 [salinity data up to levels that were unthinkable at the beginning of the mission \(Martin-Neira](#)
59 [et al. 2016, Olmedo et al., 2018; Reul et al., 2020; Boutin et al., 2022\)](#).

Formatted: Indent: Left: 0 cm, Hanging: 0,75 cm, Outline numbered + Level: 1 + Numbering Style: 1, 2, 3, ... + Start at: 1 + Alignment: Left + Aligned at: 0,63 cm + Indent at: 1,27 cm

Deleted: causing

Deleted: area coverage visible on satellite data

Deleted: The sea

Moved down [1]: (Solomon et al., 2021).

Deleted: , as reviewed in

Deleted: . (

Deleted: A recent update of the review paper showed a stabilization of the Freshwater Content (FWC) of the Arctic Basin, although observations indicate that the Beaufort Gyre keeps freshening

Deleted: , contrary

Deleted: the

Deleted: ¶

Deleted: for

Deleted: the

Deleted: maximizing

Deleted: available

Deleted: such

Deleted: or

Deleted:) among others.

Moved (insertion) [1]

Deleted: The salinity

Deleted: still

Formatted: Default Paragraph Font, Font colour: Black

Formatted: Default Paragraph Font, Font colour: Black

Formatted: Normal, Right: 0,63 cm, Border: Top: (No border), Bottom: (No border), Left: (No border), Right: (No border), Between : (No border), Tab stops: 7,96 cm, Centred + 15,92 cm, Right, Position: Horizontal: Left, Relative to: Column, Vertical: In line, Relative to: Margin, Wrap Around

82 Furthermore, the assimilation of satellite-derived SSS products using an ensemble DA
 83 method has been found to significantly improve the surface and subsurface salinity fields in
 84 the tropics (Lu et al. 2016). The advantages of assimilating three SSS products from SMOS,
 85 Aquarius (ref., Lee et al, 2012), and Soil Moisture Active Passive Mission (SMAP; e.g., Tang
 86 et al., 2017) into a global ocean forecast system using 3D-Var DA method have also been
 87 demonstrated by Martin et al (2019). Their results show the benefits of assimilating both the
 88 SMOS and SMAP datasets in the intertropical convergence zone in the tropical Pacific.
 89 However, very few studies investigated the impact of assimilating SSS products in the Arctic
 90 or high latitudes. Since the beginning, the salinity retrieval from SMOS in cold regions has
 91 been very challenging for three main reasons: i) the lower sensitivity of T_B in cold waters
 92 leading to larger SSS error (Yueh et al., 2001; e.g, the sensitivity drops from 0.5 to 0.3 K
 93 PSU^{-1} when sea surface temperature decreases from 15 to 5°C); ii) Land-sea and ice-sea
 94 contaminations resulting from abrupt changes of T_B values across these two interfaces,
 95 combined with the large ground footprint of SMOS; iii) the requirement of a well-observed
 96 steady-state period for the removal of biases. Addressing these challenges in the SMOS
 97 salinity retrieval approach, Olmedo et al. (2017) introduced a non-Bayesian retrieval method
 98 to debias the Level 1 baseline (L1B) salinity against the reference SSS from Argo data. Level
 99 1 data from the satellite is available within 24 hours, but the additional processing steps
 100 require high-quality auxiliary data so that the Level 3 and 4 SSS are only provided in delayed
 101 mode. Starting with the ESA L1B (v620) product from SMOS, the Barcelona Expert Centre
 102 (BEC) released Version 2.0 of the Arctic gridded SSS product (25 km resolution, Olmedo et
 103 al., 2018). Xie et al. (2019) evaluated the V2.0 SSS product and another gridded Arctic
 104 SMOS SSS product developed by LOCEAN (Boutin et al., 2018) during the years 2011-
 105 2013. These two SSS observations, together with an Arctic reanalysis (Xie et al., 2017) and
 106 one objective analysis product (its upgradated product is available to see Greiner et al.,
 107 2021), were validated against in-situ observations and compared with two climatology
 108 datasets: the World Ocean Atlas of 2013 (WOA2013; ref., Zweng et al., 2013) and the Polar
 109 science center Hydrographic Climatology (PHC 3.0; ref., Steele et al., 2001). They found
 110 considerable discrepancies among the different gridded SSS products, especially in the
 111 freshest seawater (<24 psu). The intercomparison of these Arctic SSS products shows room
 112 for improvement of the SMOS-based SSS in the Arctic.

114 Recently, under the framework of the ESA project Arctic+Salinity (AO/1-9158/18/I-BG), and
 115 further development of the non-Bayesian scheme (Olmedo et al., 2017), the effective
 116 resolutions of SSS data were enhanced both in space and time (Martínez et al., 2022). The

- Deleted:
- Formatted ... [4]
- Formatted ... [5]
- Deleted: there are
- Deleted: to investigate
- Deleted: impacts
- Formatted ... [6]
- Formatted ... [7]
- Formatted ... [8]
- Deleted: There are
- Deleted: for this
- Deleted:
- Formatted ... [9]
- Formatted ... [10]
- Formatted ... [11]
- Deleted:) (
- Formatted ... [12]
- Deleted: the
- Formatted ... [13]
- Formatted ... [14]
- Formatted ... [15]
- Deleted: the
- Deleted: of
- Formatted ... [16]
- Formatted ... [17]
- Deleted: and
- Formatted ... [18]
- Deleted: The removal
- Deleted: biases ideally requires
- Formatted ... [19]
- Formatted ... [20]
- Deleted: , from which climate change has deprived us
- Formatted ... [21]
- Deleted: ¶
- Formatted ... [22]
- Formatted ... [23]
- Deleted: of T_B
- Formatted ... [24]
- Deleted: the version
- Deleted: with a regular grid by
- Deleted: (e.g.,
- Formatted ... [25]
- Formatted ... [26]
- Formatted ... [27]
- Moved down [2]: 2019).
- Deleted:) via their portal (<http://bec.icm.csic.es/>; l... [28]
- Deleted: The V2 SSS regional product was produ... [29]
- Deleted: this earlier
- Formatted ... [30]
- Moved (insertion) [3]
- Formatted ... [31]
- Moved (insertion) [4]
- Formatted ... [32]
- Deleted: six
- Deleted: in the Arctic
- Formatted ... [33]
- Formatted ... [34]
- Formatted ... [35]
- Deleted: developing
- Deleted: ,
- Formatted ... [36]
- Formatted ... [37]
- Deleted: .
- Formatted ... [38]
- Formatted ... [1]

186 new version of [the](#) SSS product (V3.1) shows [the capability to monitor](#) the mesoscale
 187 structures and [river discharges](#) (e.g., [Martínez et al., 2022](#)). [This new product](#) provides daily
 188 maps ([Level 4](#)) of 9-day averages in the Arctic on [a](#) regular 25 km grid and covers a longer
 189 time period 2011-2019, [and are released through the BEC portal \(http://bec.icm.csic.es/ and](#)
 190 [also at DOI: 10.20350/digitalCSIC/12620; last accessed May 2022\)](#). The major differences in
 191 the estimation of the two SSS products (V2.0 and V3.1) are detailed in the Algorithm
 192 Theoretical Baseline Document (ATBD) of the Arctic+Salinity project (Martínez et al., 2020).
 193 [Figure 1 shows that in comparison to V2.0, V3.1 provides wider coverage in the marginal](#)
 194 [seas around the Arctic and is also fresher as indicated by the 26 psu isoline](#).
 195 The two successive versions of the BEC SMOS SSS products are assimilated [into](#) the
 196 [TOPAZ](#) Arctic reanalysis system ([detailed in Section 2](#)) during the summer of 2016. [These](#)
 197 [two assimilation runs are](#) compared to the Arctic reanalysis without assimilation of satellite
 198 SSS data, [which is identical to the product ARCTIC_REANALYSIS_PHYS_002_003](#) in the
 199 Copernicus Marine Services. The model validation against independent observations
 200 [presents](#) the differences stemming from these two SSS products, although they are from the
 201 same initial data source (SMOS). Their [impact on the assimilation](#) in [the](#) Arctic coupled ice-
 202 ocean model shows large differences, thereby [motivating](#) further efforts to improve SSS
 203 retrievals in the cold Arctic.
 204 The paper is organized as follows: Section 2 describes briefly the coupled ocean and sea ice
 205 data assimilation system and the assimilation experiments; Section 3 describes the [in-situ](#)
 206 observations and the validation metrics; [results presented in Section 4 include](#) the validation
 207 using independent SSS observations, separated into different ocean basins. Section 4 also
 208 [examines](#) the impact of SSS assimilation [on the weekly increments of other related variables](#)
 209 [near the surface](#), and explores the integrated effect on the freshwater [simulated by](#) the
 210 model. In Section 5, the findings of this study and future perspectives are summarized.
 211
 212 **2. Assimilation system and experimental design**
 213 *2.1 The Arctic ocean and sea-ice coupled data assimilation system*
 214 TOPAZ [is](#) a coupled ocean and sea ice data assimilation system, [built](#) using the
 215 [Deterministic Ensemble Kalman Filter \(DEnKF; Sakov et al., 2012\)](#) to [simultaneously](#)
 216 assimilate [multiple types of observations for](#) the ocean and sea ice (Xie et al., 2017). The
 217 ocean model in this system uses [version 2.2 of the Hybrid Coordinate Ocean Model](#)
 218 (HYCOM; Chassignet et al., 2003) with a low-distortion square grid [with a](#) horizontal
 219 resolution of 12-16 km. [The river discharge input is climatological, using the ERA-Interim](#)
 220 [runoffs channeled in a simple hydrological model, which tends to underestimate the](#)

- Deleted: advantages for monitoring
- Formatted: Font: (Asian) SimSun, Font colour: Black
- Formatted: Font: (Asian) SimSun, Font colour: Black
- Deleted: the
- Deleted: Martínez et al., 2022), and was released through the BEC portal (also at doi: 10.20350/digitalCSIC/12620; last accessed May 2022).
- Deleted: It also
- Formatted: Font: (Asian) SimSun, Font colour: Black
- Formatted: Font: (Asian) SimSun, Font colour: Black
- Formatted: ... [40]
- Deleted: days
- Deleted: the
- Formatted: Font: (Asian) SimSun, Font colour: Black
- Formatted: Font: (Asian) SimSun, Font colour: Black
- Deleted: -
- Deleted: .
- Formatted: Font: (Asian) SimSun, Font colour: Black
- Formatted: Font: (Asian) SimSun, Font colour: Black
- Deleted: Another SMOS-based Arctic surface salinity product from LOCEAN (Supply et al. 2020, Boutin et al., 2022) has been released posterior to Xie et al. (2019), but not assimilated in this study
- Formatted: Font: (Asian) SimSun, Font colour: Black
- Deleted: in...into the TOPAZ4...OPAZ Arctic reanalysis system (detailed in Section 2) during the summer of 2016, and... These two assimilation runs are compared to the Arctic reanalysis without assimilation of satellite SSS data,...which consists the Arctic reanalysis...s identical to the product ARCTIC_REANALYSIS_PHYS_002_003 in the Copernicus Marine Services at that time.... The model validation against independent observations will show...resents the differences stemming from these two SSS products, although they are originating ...rom the same initial data source (SMOS). Their effect once assimilated...mpact on the assimilation in an...he Arctic coupled ice-ocean model shows large differences, thereby also ...
- Deleted: ...situ observations and the validation metrics; The ...results are ...resented in Section 4 which includes...clude the validation using independent SSS observations, separated into different ocean basins. Section 4 also analyses...xamines the impact of the assimilation using the regional ...SS assimilation ...
- Formatted: ... [42]
- Formatted: ... [43]
- Formatted: Font: (Asian) SimSun,
- Formatted: ... [44]
- Deleted: was built as...s a coupled ocean and sea ...
- Formatted: Default Paragraph Font, Font colour: Black
- Formatted: Default Paragraph Font, Font colour: Black
- Formatted: ... [39]

315 [amplitude of the seasonal cycle and thus a saline bias at the surface \(Xie et al., 2019\)](#). The
 316 coupled sea ice model uses a single-category thermodynamic model (Drange and Simonsen,
 317 1996) [and dynamics by the modified elastic-viscous-plastic rheology \(Bouillon et al., 2013\) in](#)
 318 [an early version of the CICE model \(Lisæter et al. 2003\)](#). The model covers the whole Arctic
 319 [Ocean, \(shown in Fig. 1 in Xie et al., 2017\)](#). A seasonal inflow [of Pacific Water](#) is imposed
 320 across [the](#) Bering Strait, based on observed transports (Woodgate et al., 2012). At all lateral
 321 boundaries, the temperature and salinity stratifications are relaxed to a climatology
 322 combining version 2.0 of [WAO2013](#) and version 3.0 [of](#) PHC with a 20-grid cells buffer zone.
 323 To avoid a potential model drift, the surface salinity is relaxed to the [combined](#) climatology [as](#)
 324 [mentioned above](#), with a 30-day timescale, [but](#) the relaxation is [suppressed](#) wherever the
 325 difference from climatology exceeds 0.5 psu [to avoid the artificial formation of stable surface](#)
 326 [freshwater layers](#).

327 The two steps of the assimilation system can be translated by the following [concept](#)
 328 expressions (update and model propagation):

$$X_a = X_f + K(y - HX_f) \quad \text{---(1)}$$

$$X_f = M(X_a) \quad \text{---(2)}$$

331 Where the matrix **X** represents the model states with all 3-D and 2-D variables needed by
 332 the model forward integration, represented by the operator **M**. The subscripts 'a' and 'f'
 333 respectively indicate the analyzed model state obtained through optimization after DA and
 334 the model forecast. The vector **y** is composed of the quality-checked observations during the
 335 weekly cycle, the observation operator **H** gives the model equivalent matching the
 336 observations. The innovation term (in [parentheses](#) in Eq.1) represents the differences
 337 between the model and the various observations on the observation space. The [TOPAZ](#)
 338 [model runs an ensemble of 100 members. The K matrix \(Kalman gain\) is calculated using](#)
 339 [the ensemble covariance matrix. On a weekly basis, we use the DEnKF to assimilate](#)
 340 [different types of ocean and ice observations, including along-track sea level anomaly \(SLA\),](#)
 341 [sea surface temperature \(SST\), in-situ profiles of temperature and salinity, sea ice](#)
 342 [concentrations \(SIC\) and sea ice drift products all sourced from the Copernicus Marine](#)
 343 [Environment Monitoring Services \(CMEMS; <https://marine.copernicus.eu>\)](#). The same [TOPAZ](#)
 344 system provides a 10-[day](#) forecast of ocean physics and biogeochemistry in the Arctic
 345 [\(Bertino et al., 2021\) every day](#) via the CMEMS portal. [Like other square root versions of the](#)
 346 [Ensemble Kalman Filter, the DEnKF splits Eq. 1 into two steps: the K calculation is applied to](#)
 347 [the ensemble mean, and the anomalies are updated to match a target analysis covariance](#)
 348 [\(more details in Sakov et al., 2012\)](#).

- Moved (insertion) [2]
- Deleted:
- Deleted: combined with the
- Deleted: of
- Deleted:):
- Deleted: basin excluding the Pacific
- Deleted: .
- Moved up [3]: Zweng et al.,
- Deleted: the 2013 World Ocean Atlas (
- Deleted: WOA13;
- Deleted: 2013)
- Deleted: the Polar science center Hydrographic Climatology ...
- Deleted: (
- Formatted: Font: (Asian) SimSun, Font colour: Black
- Moved up [4]: Steele et al., 2001
- Deleted: ;
- Deleted:)
- Formatted: Font: (Asian) SimSun, Font colour: Black
- Deleted: same
- Deleted: and
- Deleted: turned off
- Deleted: . The salinity flux from
- Deleted: SSS relaxation thus spreads evenly into the mixed layer depth without creating a new
- Deleted: fresh layer at the
- Deleted: The TOPAZ model runs an ensemble of 100 members. On a weekly basis, the Deterministic Ensemble Kalman Filter (DEnKF; Sakov et al., 2012) then assimilates different types of ocean and ice observations, including along-track sea level anomaly ... [47]
- Deleted: simply
- Formatted: Font: (Asian) SimSun, Not Bold, Italic
- Deleted: ,
- Formatted: Font: (Asian) SimSun, Bold, Italic
- Deleted: parenthesis
- Deleted:),
- Deleted: as in Sakov et al. (2012)
- Deleted: updated in Xie et al. (2017).
- Deleted: TOPAZ4
- Deleted: days'
- Deleted: everyday
- Formatted: Default Paragraph Font, Font colour: Black
- Formatted: Default Paragraph Font, Font colour: Black
- Formatted

397 **2.2. Assimilation experiments and the observation error estimate for SSS**
 398 To evaluate the impact of the [assimilation of two versions of the SSS products on TOPAZ](#)
 399 [model runs](#), a control assimilation experiment (Exp0) and two parallel assimilation
 400 experiments (ExpV2, ExpV3) [for a 6-month time period \(July to December 2016\) were](#)
 401 [performed](#). Exp0 assimilates all available ocean and sea ice data, except the satellite SSS
 402 product. On the other hand, ExpV2 and ExpV3 additionally assimilate the BEC SSS [products](#)
 403 V2.0 and V3.1, respectively. [Details of the three assimilation runs are listed in Table 1.](#)
 404 [The observation error is a key parameter in any DA system: Too small values lead to](#)
 405 [overfitting, while too large values make the assimilation inefficient. The salinity errors from](#)
 406 [Passive Microwaves were previously estimated by Vinogradova et al. \(2014\); the zonal](#)
 407 [average of standard errors north of 60°N was estimated at 0.6 psu. In a recent study, Xie et](#)
 408 [al. \(2019\) evaluated the SMOS-based SSS products using in-situ observations, and revealed](#)
 409 [strong regional dependence for the V2.0 product errors; smaller than 0.4 psu in the Northern](#)
 410 [Atlantic but increasing dramatically to 1 psu in the Nordic seas and over 2 psu in the central](#)
 411 [Arctic. Undoubtedly, the salinity observation errors from Passive Microwaves are higher in](#)
 412 [high latitudes than elsewhere. Furthermore, in the Beaufort Sea \(as Fig. 12a in Xie et al.,](#)
 413 [2019\), the error of the SSS V2.0 product and the Arctic reanalysis product from TOPAZ](#)
 414 [\(same as Exp0 used in this study\) both show an inverse relationship between SSS values,](#)
 415 [and SSS errors. Hence, we use an empirical error function for ExpV2 and ExpV3 adjusted to](#)
 416 [the discrepancies as shown in Eq. 3, following Xie et al. \(2019\):](#)

$$E_{SSS} = \max \left\{ E_{int}, \left[0.6 + \frac{6}{1 + \exp\left(\frac{SSS - 16}{5}\right)} \right]^2 \right\} \quad (3)$$

417
 418 Where E_{int} is the instrumental error variance estimated by the data provider, [that part is](#)
 419 [absent from the V2.0 product. Eq. 3 yields more conservative error estimates than the](#)
 420 [providers, which also prevents the discontinuities caused by strong assimilation updates \(as](#)
 421 [an example noticed by Balibrea-Iniesta et al., 2018\). Other precautions are also applied](#)
 422 [following Sakov et al. \(2012\). By construction, the observation errors are always larger for](#)
 423 [the V3.1 than the V2.0 product, but in fresh waters they are identical. This implies that the](#)
 424 [assimilation may pull the analysis closer to the V2.0 than the V3.1 product in the more saline](#)
 425 [waters, but they are otherwise treated on equal footing, ignoring the a priori expectation that](#)
 426 [the most recent product should be more reliable.](#)

428 3. In-situ SSS observations for validation

429 All in-situ salinity profiles were collected from various repositories and cruises (as shown in
 430 Fig. 2). Salinity measurements were extracted near the surface over the Arctic domain during
 431 the experimental time period. [The sanity check procedures include: i\) location check to](#)

- Deleted: The assimilation
- Formatted ... [51]
- Deleted: ...he assimilation of two versions of the ... [52]
- Deleted: Since
- Formatted ... [53]
- Deleted: are higher in high latitudes than elsewhere,
- Formatted ... [54]
- Deleted: were previously
- Deleted: around
- Deleted: (Vinogradova
- Formatted ... [55]
- Formatted ... [56]
- Formatted ... [57]
- Deleted: ., 2014). Later on,
- Deleted: intercomparison of different
- Deleted: including the climatology, satellite,
- Formatted ... [58]
- Formatted ... [59]
- Formatted ... [60]
- Deleted: the Exp0 reanalysis showed that the ... [61]
- Formatted ... [62]
- Deleted: are often higher in areas of fresher water,
- Deleted: quantitatively they combine
- Formatted ... [63]
- Deleted: errors of
- Formatted ... [64]
- Deleted: remote sensing products, models
- Formatted ... [65]
- Deleted: climatologies
- Formatted ... [66]
- Formatted ... [67]
- Deleted: may be larger than the remote sensing
- Deleted: alone. Still
- Formatted ... [68]
- Formatted ... [69]
- Deleted: 3:
- Formatted ... [70]
- Deleted: δ_{SSS}
- Deleted: δ_{int}
- Deleted: δ_{int}
- Deleted: . In ExpV2, it... that part is set to zero du... [71]
- Formatted ... [72]
- Deleted:
- Formatted ... [73]
- Deleted: ...situ salinity profiles were collected fro... [74]
- Formatted ... [48]
- Formatted ... [49]
- Formatted ... [50]

539 ensure observation in the water grid same as the model used; ii) omit the invalid profiles if
540 the top depth is deeper than 8 m; iii) remove redundant observations. Since the model does
541 not reproduce local gradients of the vertical salinity profiles shown in Supply et al. (2020), all
542 the salinity profiles are averaged over the upper 8 meters below the surface. This also avoids
543 the loss of the profiles that do not reach the surface.

544 • *Data from the Beaufort Gyre Experiment Project (BGEP)*

545 The BGEP has maintained an observing system in the Canadian Basin since 2003 and
546 provides in-situ observations over the Beaufort Gyre every summer. Although the BGEP has
547 maintained three bottom-tethered moorings since 2003, the shallowest depth of the
548 measured profiles for temperature and salinity is below 50 m. Hence, in this study, we only
549 use the Conductivity Temperature Depth (CTD) dataset from the cruise in 2016
550 (<https://www2.whoi.edu/site/beaufortgyre/data/ctd-and-geochemistry/>, last access: 14th
551 February 2022). SSS observations from these CTD profiles in the time period from 13th Sep
552 to 10th Oct 2016 are represented by the red triangles in Fig. 2.

553 • *Data from Oceans Melting Greenland (OMG)*

554 The project Oceans Melting Greenland was funded by NASA to understand the role of the
555 ocean in melting Greenland's glaciers. Over a five-year campaign, this project collected
556 temperature and salinity profiles by Airborne eXpendable Conductivity Temperature Depth
557 (AXCTD) launched from an aircraft (e.g., Fenty, et al, 2016). The deployed probe can sink to
558 a depth of 1000 meters, connected with a float by a wire. The measured temperature and
559 conductivity are then sent back to the aircraft. These salinity profiles collected during the first
560 OMG campaign in 2016 are downloaded from
561 https://podaac.jpl.nasa.gov/dataset/OMG_L2_AXCTD/ (last access: 10th February 2022). The
562 SSS from OMG distributed around Greenland, from 13th Sep to 10th Oct 2016 are shown as
563 the inverted blue triangles in Fig. 2.

564 • *Data from the International Council for the Exploration of the Sea (ICES)*

565 Salinity profiles were also obtained from the ICES portal (<https://www.ices.dk>). Shown as
566 blue squares in Fig. 2, the locations of the profiles during the last 6 months of 2016 are
567 dense in the Nordic Seas and restricted to north of 58°N for this study. Valid salinity profiles
568 from ICES (last access: 9th February 2022) are obtained from 6th July to 23rd Nov in 2016.

569 • *Data from other cruises at the Arctic Data Center (ADC)*

570 Surface salinity observations from scientific cruises are obtained from the Arctic Data
571 Center portal (<https://arcticdata.io/catalog/data>; last access: 17th Feb 2022). During the
572 model experiment, the first relevant cruise in ADC was SKQ201612S which was operated by
573 University of Alaska Fairbanks with the RV Sikuliaq. This cruise collected data from Nome,

Formatted: Outline numbered + Level: 1 + Numbering
Style: Bullet + Aligned at: 0,63 cm + Indent at: 1,27 cm

Deleted: -

Deleted: 1

Formatted: Outline numbered + Level: 1 + Numbering
Style: Bullet + Aligned at: 0,63 cm + Indent at: 1,27 cm

Formatted: Font: (Asian) SimSun, 11 pt

Deleted: ,

Deleted: red-

Deleted: 1

Formatted: Font: (Asian) SimSun, 11 pt

Formatted: Outline numbered + Level: 1 + Numbering
Style: Bullet + Aligned at: 0,63 cm + Indent at: 1,27 cm

Deleted: 1

Deleted: ,

Deleted: the

Formatted: Font: (Default) Arial, (Asian) SimSun

Deleted: ,

Formatted: Outline numbered + Level: 1 + Numbering
Style: Bullet + Aligned at: 0,63 cm + Indent at: 1,27 cm

Formatted: Default Paragraph Font, Font colour: Black

Formatted: Default Paragraph Font, Font colour: Black

Formatted: Normal, Right: 0,63 cm, Border: Top: (No border), Bottom: (No border), Left: (No border), Right: (No border), Between : (No border), Tab stops: 7,96 cm, Centred + 15,92 cm, Right, Position: Horizontal: Left, Relative to: Column, Vertical: In line, Relative to: Margin, Wrap Around

583 Alaska on 3rd September, to the northeast Chukchi Sea, and then back to Nome at the end of
 584 September 2016. The temperature and salinity profiles were collected by a Sea-Bird 911
 585 CTD instrument package. All measurements at each station were done both down- and up-
 586 cast ways. To produce water column profiles at each station, the down-cast data were
 587 binned at 1 m intervals (Goñi et al., 2021). Besides the CTD profiles of SKQ201612S, more
 588 seawater samples were collected via the surface underway system on the RV Sikuliaq.
 589 Through a sea chest below the waterline (e.g., 4-8 m), the uncontaminated seawater was
 590 pumped into the ship and the corresponding filtration system supplies samples every 3 hours
 591 to the sensors (More details in Goñi et al., 2019). These SSS observations were obtained on
 592 the 9th, 27th of September, indicated as blue crosses in Fig. 2.
 593 Moreover, SSS measurements were also collected from the Seabird CTD on board Sir
 594 Wilfrid Laurier (SWL), but only in July 2016. This cruise is part of the annual monitoring from
 595 the Canadian Coast Guard Service (Cooper et al., 2019). The SSS observations are
 596 obtained near the Bering Strait close to the Pacific boundary of our model.
 597 After skipping the diurnal signals in observed surface salinity, all valid SSS measurements
 598 from the above data sources are compared with the daily average SSS of the three
 599 assimilation experiments listed in Table 1. All the assimilation runs use a weekly assimilation
 600 cycle: The model runs forward 7 days after each assimilation step and provides daily
 601 averages for each day from the ensemble mean, which we refer to as “forecast” even when
 602 using delayed-mode observations and atmospheric forcings. The model data has been
 603 collocated with the observations for validation. To estimate the forecast differences to
 604 observations, we use the standard statistical moments:

$$Bias = \frac{\sum_{i=1}^N \sum_1^{O_i} (HX_i - y_i)}{\sum_{i=1}^N O_i} \quad (4),$$

$$RMSD = \sqrt{\frac{\sum_{i=1}^N \sum_1^{O_i} (HX_i - y_i)^2}{\sum_{i=1}^N O_i}} \quad (5),$$

607 Where i is the i th day, O_i represents the number of observations on this day, and N
 608 represents the total number of days depending on the source of observations. Then X_i
 609 represents the model daily average at the observation time as the ensemble means of 100
 610 model members. H is an operator to extract the SSS simulation from the model at the
 611 observed location. The model performance can then be quantitatively compared between the
 612 three assimilation runs.
 613 In addition, we further introduce a two-sample Student's t-test to evaluate the significance of
 614 the change of SSS bias in ExpV2/ExpV3 with respect to Exp0. Compared to in-situ
 615 observations, the SSS misfits in Exp0 are the error array e_1 . The corresponding error array

Deleted:

Deleted: eg

Deleted: from

Deleted: to

Deleted: 1

Deleted:) vessel

Deleted:

Deleted: removing

Deleted: effect of

Deleted: cycle

Deleted: the

Deleted: $\frac{1}{N} \sum_{i=1}^N (HX_i - y_i)$

Deleted: $\frac{1}{N} \sum_{i=1}^N (HX_i - y_i)^2$

Deleted:

Deleted: , and X_i

Formatted: Font: (Asian) SimSun, 12 pt

Deleted: time of the

Deleted: y_i . The X_i bar denotes

Deleted: mean using

Deleted: here, and the

Deleted: H extracts

Deleted: SSS

Deleted: among

Formatted: Font: (Asian) SimSun, Not Italic, Not Highlight

Formatted: Default Paragraph Font, Font colour: Black

Formatted: Default Paragraph Font, Font colour: Black

Formatted: Normal, Right: 0,63 cm, Border: Top: (No border), Bottom: (No border), Left: (No border), Right: (No border), Between : (No border), Tab stops: 7,96 cm, Centred + 15,92 cm, Right, Position: Horizontal: Left, Relative to: Column, Vertical: In line, Relative to: Margin, Wrap Around

638 from ExpV2 or ExpV3 is called e_2 . Thus, considering the null hypothesis $H_0: e_1$ and e_2 are
639 the means of indiscernible random draws, the t-value can be calculated as follows:

$$t = \frac{|e_2 - e_1|}{\sqrt{s_1^2/(n_1 - 1) + s_2^2/(n_2 - 1)}}$$

641 Where s_1 (s_2) is the standard deviation in the e_1 (e_2), and n_1 (n_2) is the number of observations.
642 For every t-value, the p-value from the above equation is the probability that random errors
643 would prove H_0 wrong. Low p-values (<0.05) indicate that the change of bias due to
644 assimilation is significant.

645 4. Results

646 4.1 Diagnosing using assimilation statistics

647 The SSS innovations in the two assimilation runs, ExpV2 and ExpV3, are compared in Fig. 3,
648 together with the number of assimilated SSS observations and the ensemble spread
649 calculated by the ensemble standard deviation. The total number of observations is at its
650 maximum in September when the sea ice cover is minimal. Since both versions of the SSS
651 product share the same time frequency (9-day average) and gridded format, the number of
652 assimilated observations in the two runs remains identical (gray lines in Fig. 3). For ExpV2,
653 the Root Mean Square (RMS) of the SSS innovation varies between 0.4 and 1.2 psu, but the
654 mean of SSS innovation, calculated as the observation minus the model simulation (cf. the
655 bracket in Eq. 1), shows the saline bias of 0.4 psu, highest in September. However, in ExpV3
656 the salinity bias quickly disappears after a few data assimilation cycles. The RMS of the SSS
657 innovation is larger in ExpV3 between 0.6 and 1.6 psu, which can partly be explained by the
658 higher effective resolution of the V3.1 product and the double penalty effect. In ExpV3, the
659 RMS of the SSS innovation (the red line) jumps down after the first SSS assimilation step.
660 The RMS of SSS innovations and the observation errors both decrease from summer to
661 winter, following a seasonal cycle as the areas of fresher water get gradually ice-covered.
662 The domain-averaged observation errors are only slightly larger in ExpV3 than in ExpV2, as
663 explained above, and the RMS of SSS innovations become lower than the observation errors
664 near the end of the run, which indicates that the observation errors for the V2.0 SSS have
665 been overestimated.
666 In the top panels of Fig. 4, the SSS maps present the control run (Exp0) in August and
667 September 2016, respectively. For Exp0 in August, low salinity waters are found in the
668 Beaufort Sea near the Mackenzie River and along the East Siberian coast. In September, the
669 fresher waters, below 30 psu, bridge the two areas in Exp0 probably due to sea ice melt,
670 although the lowest salinity near the Siberian coast remains unchanged from August to
671 September (as indicated by the 28 psu isoline). Compared with the SSS observations from
672

Formatted: Font: (Default) Arial, (Asian) SimSun

Formatted: Indent: Left: 0 cm, Hanging: 0.75 cm, Outline numbered + Level: 1 + Numbering Style: 1, 2, 3, ... + Start at: 1 + Alignment: Left + Aligned at: 0,63 cm + Indent at: 1,27 cm

Formatted: Outline numbered + Level: 2 + Numbering Style: 1, 2, 3, ... + Start at: 1 + Alignment: Left + Aligned at: 0,63 cm + Indent at: 1,27 cm

Deleted: ,

Deleted: ,

Deleted: shown

Deleted: 2

Formatted: Font: (Asian) SimSun, Not Italic

Deleted: of SSS

Deleted:

Deleted: days

Deleted: are

Deleted: 2

Formatted: Font: (Asian) SimSun,

Deleted: which is

Deleted: opposite of

Deleted: bias (Eq. 1)

Deleted: a positive salinity bias, especially during September, when the ...

Deleted: is around

Deleted: .

Deleted: are

Deleted: .

Deleted: yearly

Deleted: observations

Deleted: sound

Deleted: Figure 3 shows

Deleted: from the two SSS assimilation runs (ExpV2 and ExpV3) and...

Deleted: during

Deleted: .

Deleted: In

Deleted: low saline

Deleted: Both in ExpV2 and ExpV3, the low salinity areas are even fresher during the two months compared to Exp0. Notably, the areas of salinity lower than 28 psu are broader in ExpV3. On the European side of the Arctic, the characteristics of the saline Atlantic water are very similar in all the three runs (as shown by the isolines of 34 and 35 psu in Fig. 3). (... [76])

Formatted: Default Paragraph Font, Font colour: Black

Formatted: Default Paragraph Font, Font colour: Black

Formatted

... [75]

722 SMOS (Fig. 1), these two low salinity waters are clearly underestimated in Exp0. Meanwhile,
 723 the relatively saline 32 psu isoline crosses both the Eurasian basin and the Baffin Bay. In the
 724 Laptev Sea, due to the significant effects of river runoff and ice melt, the salinity shows a
 725 strong gradient from the southeast to the northern part. During winter, the salinity increases
 726 to 34 psu, and decreases in summer near to 30 psu (Janout et al., 2017). In the northwest
 727 Laptev Sea, the saline tongue of 32 psu extends eastward to Taymyr Peninsula (TP), North
 728 of the TP, the Kara Sea freshwater meets with the Atlantic Water pathways from the Fram
 729 Strait and Barents Sea (shown in Figure 1 by Janout et al., 2017). Close to the TP, the
 730 observations at the mooring profiles in Janout et al. (2017) show much fresher surface
 731 salinity (29 psu) than the subsurface salinity (32 psu) in summer. Compared to the SMOS
 732 SSS maps (Fig. 1), only the V3.1 product shows the 32 psu isolines around the TP. Another
 733 difference between the two SMOS products arises in the Chukchi Sea where the V3.1
 734 product is more saline than both the V2.0 product and SSS in Exp0.
 735 Then the middle and bottom panels of Fig. 4 show the SSS differences in August and
 736 September 2016 between the SSS assimilation runs and the control run. Fig. 4c and 4d both
 737 show a freshening of the coastal areas in the Kara Sea, Laptev Sea, and East Siberian Sea,
 738 but in ExpV3 the freshening is stronger and wider (Fig. 4e and 4f). In the Beaufort Sea,
 739 ExpV2 mainly brings a local freshening near the mouth of the Mackenzie River in August,
 740 which then spreads out along the coast in September. The freshening in the BS brought by
 741 ExpV3 affects a broader area, even including the Canadian Archipelago. ExpV3 also
 742 freshens the SSS on both sides of Greenland Island. From August onwards, the SSS in
 743 ExpV3 freshens by over 1 psu along the whole east Greenland coast, which clearly does not
 744 happen in ExpV2. In fact, the 32 psu isoline in ExpV3 (not shown) extends hundreds of
 745 kilometers further to the South East Greenland coast in comparison to Exp0 and ExpV2. The
 746 rest of the Greenland coast is also fresher by 0.5 psu in ExpV3 during both months. This is a
 747 sign of a consistent change in the V3.1 product.
 748 Even though most of the SSS assimilation leads to a freshening of the surface, a few
 749 locations show higher salinity than Exp0, these are different from ExpV2 to ExpV3. For
 750 example, the saline increment near the Bering Strait is larger in ExpV3 in excess of 1 psu,
 751 consistently with the difference between the two remote sensing products (Fig. 1).
 752 Other increases in SSS concern small areas near estuaries and are more common in ExpV3.
 753 The increase to the west of the Yamal Peninsula can be explained by a model setup bias in
 754 the location of the Ob river but compensated by the SSS assimilation. In the above
 755 comparisons of SSS maps, the central Arctic is not discussed, since the region is covered by
 756 sea ice and the effect of assimilation is indirect.

Deleted: Exp0,

Deleted: 32 psu salinity

Deleted: In ExpV2, the salinity tongue extends eastwards but is narrower, but in ExpV3 it remains to the West of Severnaya Zemlya.

Deleted: of

Deleted: This motivates the assimilation of the SSS products to compensate for the paucity of in-situ observations...

Moved (insertion) [5]

Deleted: The 32 psu isoline in ExpV3 extends hundreds of kilometers further South along east Greenland in comparison to Exp0 and ExpV2. The change between simulations is larger than the differences between August and September. Another area of notable differences is in the northern Baffin Bay. In ExpV3, the area above 32 psu is shrunken to the South of Nares Strait under the assimilation of the V3.1 SSS product, which may compensate for the lack of mass loss from the Greenland ice sheet in the model. ¶ In the

Formatted: Font: (Asian) SimSun, Font colour: Auto

Formatted: Indent: First line: 0 cm

Deleted: excluded

Deleted: can only be

Formatted: Default Paragraph Font, Font colour: Black

Formatted: Default Paragraph Font, Font colour: Black

Formatted: Normal, Right: 0,63 cm, Border: Top: (No border), Bottom: (No border), Left: (No border), Right: (No border), Between : (No border), Tab stops: 7,96 cm, Centred + 15,92 cm, Right, Position: Horizontal: Left, Relative to: Column, Vertical: In line, Relative to: Margin, Wrap Around

780 4.2 Comparison with independent *in-situ* observations
 781 [Quality-checked in-situ](#) observations in the Central Arctic are very unevenly distributed. [After](#)
 782 pooling all [platforms](#) together, we further investigate the SSS misfits [in](#) six subregions of the
 783 Arctic (Fig. 2 and Table 2). This section will present statistics of differences to independent
 784 *in-situ* observations, [separately](#) considering marginal seas.

786 [Beaufort Sea \(BS\)](#); Figure 5 shows the scatterplots of SSS in the three runs against *in-situ*
 787 observations from BGEP, OMG, and ICES. In the Beaufort Sea (top panel in Fig. 5), the
 788 observed SSS varies in a range of 26-29 psu. The range of SSS in Exp0 is much smaller,
 789 between 29-31 psu with a saline bias of 2.6 psu and an RMSD of 2.7 psu, but otherwise, [it](#)
 790 [shows](#) a reasonably linear relationship ($r=0.59$). The SSS bias in Exp0 has the same value
 791 as in Xie et al. (2019), although estimated using the BGEP observations in a different time
 792 period (2011-2013). The range of SSS in ExpV2 is slightly improved to 28-30.5 psu. [Further](#),
 793 [the](#) bias [is reduced](#) by 0.5 psu, corresponding to bias and RMSD reductions of respectively
 794 13.5% and 10.5% with respect to Exp0. In ExpV3, the SSS range is much closer, between
 795 26.5 and 30.5 psu, [and the resulting bias and RMSD reductions of SSS](#) are respectively
 796 26.3% and 17.3% with respect to Exp0. [Both the bias reduction in ExpV2 and ExpV3 relative](#)
 797 [to Exp0 pass the significance test \(\$\alpha = 0.05\$ \) through Student's t-test.](#) Furthermore,
 798 compared [to all in-situ SSS in BS \(top panels in Fig. 7\)](#), the SSS misfits in ExpV3 [show](#) a
 799 [stronger](#) reduction [by](#) 26.0% for bias and 20.6% for RMSD. ExpV2 [reduces these errors by](#)
 800 [half as much](#) (13.5% for bias and 11.5% for RMSD). These results clearly indicate that the
 801 new version of the SSS [is more beneficial for data assimilation](#) in the Beaufort Sea.

803 [Chukchi Sea \(CS\)](#); Fig. 6 shows the SSS deviations as a function of time during the SKQ
 804 cruise route. [Figure 6a shows the surface levels from CTDs](#). The saline bias (2.8 psu) is
 805 more pronounced than in the Beaufort Sea, [which we attribute to the proximity to the model](#)
 806 [boundary](#) in the Bering Strait, [relaxed to climatological values](#), where the interannual
 807 variability of Pacific water is not included. After assimilating SSS products, a reduction of the
 808 bias is observed during September, by 15.5% in ExpV2 and up to 22.2% in ExpV3. [The](#)
 809 comparison to underway surface water samples (Fig. 6b) also shows [an error reduction of](#)
 810 around 15%, though [fewer](#) differences between ExpV2 and ExpV3.
 811 [Considering other cruise data in the CS \(Fig. 7; bottom panels\)](#), the SSS in Exp0 shows
 812 [almost uniform values](#) with a saline bias [of](#) about 2.3 psu and [an](#) RMSD [of](#) 2.6 psu. A recent
 813 observational study by Goñi et al. (2021) shows that the surface salinity of [the](#) CS during late
 814 summer varies [between](#) 28-30 psu during [the](#) time period 2016-2017. [The range of SSS](#)
 815 observations [considered here is slightly broader](#) (27-32 psu). [The](#) assimilation of SSS

- Deleted:
- Formatted ... [80]
- Deleted: Valid
- Deleted: When...fter pooling all observation ... [82]
- Formatted ... [81]
- Deleted: :
- Deleted: 4
- Deleted:
- Formatted ... [83]
- Formatted ... [84]
- Formatted ... [85]
- Formatted ... [86]
- Deleted: which are respectively obtained
- Deleted: 4
- Formatted ... [87]
- Formatted ... [88]
- Deleted: show
- Deleted: .
- Formatted ... [89]
- Formatted ... [90]
- Deleted: of
- Deleted: .
- Deleted: , a
- Formatted ... [91]
- Formatted ... [92]
- Formatted ... [93]
- Deleted: reduction
- Formatted ... [94]
- Deleted: around
- Formatted ... [95]
- Deleted: so
- Deleted: in ExpV3
- Formatted ... [96]
- Formatted ... [97]
- Formatted ... [98]
- Deleted: with the combined SSS observations shown
- Deleted: the upper of
- Deleted: 6,
- Deleted: have
- Formatted ... [99]
- Formatted ... [100]
- Formatted ... [101]
- Formatted ... [102]
- Deleted: robust
- Deleted: of
- Deleted: There is also a reduction in
- Deleted: of
- Formatted ... [103]
- Formatted ... [104]
- Formatted ... [105]
- Deleted: , but smaller in comparison with ExpV3.
- Deleted: assimilating
- Formatted ... [106]
- Formatted ... [107]
- Formatted ... [108]
- Deleted: efficient to improve the SSS
- Formatted ... [109]
- Deleted: :...(CS): Fig. 5... shows the SSS deviat... [110]
- Deleted: Furthermore, compared with ...onsideri... [111]
- Formatted ... [77]
- Formatted ... [78]
- Formatted ... [79]

944 products, reduces the misfits (bias and RMSD). As in the BS, the SSS in ExpV3 has more
 945 significant reductions in bias (17.7%) and RMSD (16.4%). After assimilation, the deviations
 946 are in the same range as found in the BS. All the bias reductions in ExpV2 and ExpV3 are
 947 significant compared to Exp0 through the t-test ($\alpha = 0.05$).
 948
 949 Greenland Sea (GS): Most SSS observations around Greenland are from the OMG
 950 programme, shown as the blue downward triangles in Fig. 2. Considering first all SSS
 951 observations from OMG, the SSS misfits in the three runs (shown in the middle panels of Fig.
 952 5) show smaller bias and RMSD than in the BS and the CS. However, the SSS in ExpV3 still
 953 brings significant error reductions with a reduction of 32.6%/9.4% of the bias and RMSD
 954 compared to Exp0. Notably, the SSS misfits in ExpV2 are almost identical to Exp0, which
 955 indicates that the V2.0 SSS product was not informative there,
 956 We now separate the evaluation in the East and West of Greenland covering the GS and
 957 Baffin Bay (BB) areas as shown in Fig. 2 (also listed in Table 2). The top panel of Fig. 8
 958 shows that all SSS observations available in the GS vary between 27 and 35 psu. This large
 959 range includes fresh coastal waters, Arctic water, and Atlantic Water. The three assimilation
 960 runs show different saline biases, especially for salinities lower than 30 psu. While in
 961 observations the minimum salinity is below 28 psu, it only reaches 30 psu in ExpV3, and 31
 962 psu in both Exp0 and ExpV2. As a result, the bias reduction in ExpV3 is over 50% and the
 963 RMSD decreased by about 10.5% in the GS. ExpV2 is disappointingly similar to Exp0. This
 964 is also the case in BB (shown in Fig. 8 bottom row), where differences between ExpV2 and
 965 Exp0 are less than 0.02 psu. In contrast, ExpV3 reduces the SSS bias, but does not
 966 significantly reduce the RMSD in the BB. One possible explanation is the double-penalty
 967 effect because the V3.1 product has a higher effective resolution than V2.0. This can be
 968 seen in Fig. 8 as the ExpV3 values are more scattered.
 969 Finally, we examine the SSS deviations in the Barents Sea and the Norwegian Sea. The
 970 SSS bias and RMSD are the lowest in ExpV3 in Table 2, even though the reductions are not
 971 as significant as in the area of fresher surface waters. Compared to the ICES observations
 972 distributed in the North Atlantic and the Nordic Seas (blue squares in Fig. 2), the scatterplots
 973 of Exp0 and ExpV2 are nearly identical (see the bottom panels in Fig. 5). The minimum
 974 salinity in these two runs is 32 psu. The SSS bias and RMSD in both runs are also similar
 975 (differences less than 0.01 psu). In contrast, lower salinity values are found in ExpV3, below
 976 32 psu, although the saline bias remains around 0.5 psu on average. Notably, the SSS in
 977 ExpV3 shows that data assimilation can reduce the bias by 15% compared to Exp0, but the
 978 RMSD only reduced about 0.03 psu, also possibly due to the double penalty effect. This also

- Deleted: , the two runs of Exp V2 and ExpV3, sh... [115]
- Deleted: : Around Greenland, most...(GS): Most... [116]
- Deleted: To better understand
- Deleted: changes caused by
- Deleted: SSS assimilation
- Deleted: potential dependence on the localizatio... [120]
- Formatted ... [117]
- Formatted ... [118]
- Formatted ... [119]
- Formatted ... [121]
- Deleted: where the involved observations are
- Deleted: 1
- Deleted: these two regions are
- Deleted: as S5 and S6
- Deleted: As shown in the
- Deleted: 7, the
- Formatted ... [122]
- Formatted ... [123]
- Formatted ... [124]
- Formatted ... [125]
- Formatted ... [126]
- Formatted ... [127]
- Deleted: SSS variation reflects the real condition... [128]
- Formatted ... [129]
- Deleted: and the fresh coast water converge wit... [130]
- Formatted ... [131]
- Deleted: less
- Formatted ... [132]
- Deleted: lower than
- Deleted: is around
- Formatted ... [133]
- Formatted ... [134]
- Deleted: Correspondingly
- Deleted: with
- Formatted ... [135]
- Formatted ... [136]
- Deleted: Notably, no clear changes for SSS in
- Deleted: are found in comparison with
- Deleted: As indicated from SSS scatterplots of
- Formatted ... [137]
- Formatted ... [138]
- Deleted: three runs
- Deleted: S6 in Table 1, also
- Deleted: panels of Fig. 7), there are no clear
- Formatted ... [139]
- Formatted ... [140]
- Formatted ... [141]
- Formatted ... [142]
- Deleted: (
- Deleted:). On the other hand, w.r.t ExpV2 and Exp0,
- Deleted: registers a reduction of
- Formatted ... [143]
- Formatted ... [144]
- Formatted ... [145]
- Deleted: , even has no significant reduction of th... [146]
- Formatted ... [147]
- Deleted: ¶ [148]
- Formatted ... [112]
- Formatted ... [113]
- Formatted ... [114]

1128 suggests that the improvements near the coast will be the next challenge for future versions
1129 of the SSS product.

1130 ▲
1131 4.3 Impact analysis of SSS assimilation

1132 The above section has demonstrated that the assimilation of remote sensing SSS generally
1133 improves the match to independent in-situ measurements, although the improvements are
1134 location-dependent. Since large areas are void of in-situ measurements, the increment
1135 changes of other surface variables caused by assimilation from the three runs will also be
1136 meaningful in understanding the impacts incurred. The increments are the differences
1137 between the analysis and the forecast. The calculation of them is the result of the innovations
1138 of all assimilated observations multiplied by the Kalman gain, as computed in Eq. (1). Since
1139 the DEnKF update is multivariate, we present the impact of the assimilation on other model
1140 variables closely related to the SSS: SST and SIC. Since the only difference in the setting
1141 between the three runs is the assimilation of SSS, we can attribute the differences to the
1142 impact of SSS observations. In theory, if both the model and observations were unbiased,
1143 the increments of other assimilated variables should generally decrease because of the
1144 presence of a new SSS term in the denominator of the Kalman Gain (the assimilated
1145 observations compete with each other), but SSS biases can also spill over the other model
1146 variables and increase the innovations on the following assimilation step and thus the
1147 resulting increments. Hypothetically, if the SSS were the only source of errors in TOPAZ, the
1148 increments of other variables should vanish over time. Figure 9 compares the time-averaged
1149 increments of SIC and seawater temperature in the top 3-m layer (considered as SST here)
1150 in the three runs. The sign of the increments remains overall the same across the three
1151 experiments, both for SST and SIC. The SST increments in the three runs are negative in the
1152 open ocean and positive near the ice edge, as shown in the right column of Fig. 9. ▲

1153 The SST increments in Exp0 and in ExpV2 are nearly identical, but in ExpV3 there are few
1154 areas such as in the Kara Sea and in the Laptev Sea where the SST increments have been
1155 suppressed. These are locations where the SSS and SST are positively correlated, so the
1156 updated SSS by assimilation is also helpful in reducing the water temperature misfits near
1157 the surface. The changes in SST are however small with respect to the large SSS
1158 differences in Figure 4. In Exp0, the SIC increments are small (<5%) inside the ice pack. The
1159 satellite SIC observations are assimilated every week and help to correctly position the ice
1160 edge (Sakov et al., 2012). The increments exceed 5% along the ice edge, as can be seen in
1161 the northern Barents Sea.

1162 The assimilation of the V2.0 SSS product also shows minimal differences from Exp0 partly
1163 because of the conservative sea ice mask in the V2.0 SMOS SSS. The SIC increments are

Deleted: how to improve the fresh salinity measurements

Deleted: coastline around the Nordic Seas

Deleted: the SSS retrieve after the V3.1

Formatted: Font: (Default) Arial, (Asian) SimSun

Deleted: the SSS

Formatted: Font: (Asian) SimSun, Not Italic, Font colour: Auto

Formatted: No bullets or numbering

Formatted: Font: (Asian) SimSun, Not Italic

Deleted: Above quantitative validation of SSS against various observations, shows that the assimilation of these two satellite products brings many positive benefits to constrain the simulated SSS not too far from real conditions, although the improvements are quite dependent on the locations. Surface salinity changes in the three runs (Fig. 8) contrasts the averaged increment of SSS in 2016. The increment means the difference between the analysis model state and the previous forecast model state, and represents the model correction of SSS by DA. As a control reference, the SSS increment in Exp0 is mainly in the river mouths, such as those around the Lena River (LR) and the Yenisey River (YR), while in open ocean it is extremely small. This is an indication that the presently assimilated observations in Exp0 are not able to correct the surface salinity very much. Assimilation of version 2.0 SSS product (Fig. 8b) shows four dominant areas around the central Arctic with negative increment in SSS. Two of them are in the Kara Sea (KS) and the East Siberian Sea (ESS). These are regions where the model has an underestimation for the affected extent of the freshwater impulse around rivers. The third region, the southern Laptev Sea (LS), is found to be further separated into two small areas. The fourth region is along the coastline in Beaufort Sea. On the contrary, a positive increment in SSS is found in the Hudson Bay (HB), outside the central Arctic. In comparison to ExpV2, except for the wide negative SSS increment area around ESS, much more areas are found with the different incremental patterns in ExpV3 (Fig. 8c). Two strong positive SSS increment centers appear around the Kara Sea and the north of LS, which is clearly different from the increment pattern in ExpV2. The difference is likely due to the processing of the two versions of the SSS products using different climatologies (Martínez et al., 2022). The two nearby regions (BS coast and HB) with negative SSS increment regions in ExpV2 are found to form a dipole of negative and positive increment regions in ExpV3. This pattern is likely due to the benefits of the increase in the horizontal resolution in the newest version (... [149])

Formatted: Default Paragraph Font, Font colour: Black

Formatted: Default Paragraph Font, Font colour: Black

Formatted: Normal, Right: 0,63 cm, Border: Top: (No border), Bottom: (No border), Left: (No border), Right: (No border), Between : (No border), Tab stops: 7,96 cm, Centred + 15,92 cm, Right, Position: Horizontal: Left, Relative to: Column, Vertical: In line, Relative to: Margin, Wrap Around

1255 opposite to those of SST, showing that the assimilation warms the surface water where ice is
 1256 removed, which is consistent with Lisæter et al. (2003). Only minor differences between
 1257 ExpV2 and ExpV0 are visible along all areas swept by the ice edge during the 6-month
 1258 experiment, for example in the Kara Sea. In contrast, the assimilation of the V3.1 SSS
 1259 product shows larger changes of SIC increments than in ExpV2 with a broader area of
 1260 negative increments (removed ice) in the northern Barents Sea. This is not visibly related to
 1261 the SST increments but to the freshening caused by the assimilation of V3.1 SSS as SSS
 1262 and SIC are positively correlated in the northern Barents Sea, as shown by Fig. 2 in Sakov et
 1263 al. (2012). The increased SIC increments may be an indication that the SSS freshening could
 1264 be excessive.

1265 Since the whole water column is updated by the assimilation, the freshwater content is also
 1266 modified by the assimilation of SSS. There are however complex relationships between SSS
 1267 and FWC as shown by Fournier et al. (2020). The changes in FWC in the Arctic are
 1268 calculated as in Eq. (6) derived from Proshutinsky et al. (2009), although this method was
 1269 initially intended for the BS. Applying the same formula for interpolation of in-situ
 1270 observations, Proshutinsky et al. (2020) estimated the time-averaged summer freshwater
 1271 content in the Beaufort Gyre region in two time periods (1950-1980 and 2013-2018). In the
 1272 latter period, they located the FWC centre in the BS around (150°W, 75°N) and drew the 20-
 1273 m isoline over more than 5 degrees of latitude and nearly 30 degrees of longitude on
 1274 average. When compared to the earlier reference period, the FWC in the BS has increased
 1275 and its centre has shifted westward.

1276 Following Proshutinsky et al. (2009), the model FWC in the Arctic is estimated as:

$$FWC = \int_{z_0}^{z_{ref}} (1 - \frac{S(z)}{S_{ref}}) dz \quad (6)$$

1277 Where the reference salinity value S_{ref} is taken at 34.8 psu, z_{ref} is the depth of the reference
 1278 salinity or the sea bed, and $S(z)$ is the salinity profile. Figure 10 shows the FWC on two
 1279 representative days, September 20th and October 20th, 2016. In Exp0, the reanalysis
 1280 reproduces the typical FWC distribution in the Arctic with a maximum in the Beaufort Sea.
 1281 The 20 m isolines in Fig. 10a and 10d show an increase in spatial coverage during October,
 1282 consistent with Rosenblum et al. (2021), but the 20 m isoline is not extending as far as 170°E
 1283 compared to Proshutinsky et al. (2020). After assimilation of SSS products (either V2.0 or
 1284 V3.1), the amplitude and the spatial distribution of the FWC maximum increase slightly in the
 1285 BS (see Fig. 10b and 10c). A much larger increase of FWC appears on the East Siberian
 1286 shelf and in the coastal areas of the Laptev Sea and eastern Kara Sea, although to a
 1287 different extent in ExpV2 and in ExpV3. In the eastern Kara Sea, the FWC increases over a
 1288 wider area in ExpV2 than in ExpV3. To the west of the Yamal Peninsula, ExpV3 shows a

- Moved up [5]: Fig. (... [154])
- Deleted: 8c, significantly different to that in Exp0 (... [153])
- Formatted (... [153])
- Deleted: for...n two time-period (1950s-1980s... (... [155])
- Formatted (... [156])
- Deleted: covers...ver more than 5 degrees of lat (... [157])
- Deleted: Correspondingly, referring to Eq. 6, (... [158])
- Deleted: reaching to 34.8 psu. Figure 9 ...f the re (... [159])
- Deleted: , respectively... In Exp0, the reanalysis (... [161])
- Formatted (... [160])
- Deleted: region and
- Deleted: dominant centre located...aximum in th (... [164])
- Formatted (... [162])
- Formatted (... [163])
- Deleted: FWCL
- Deleted: 9a
- Formatted (... [166])
- Formatted (... [167])
- Formatted (... [168])
- Formatted (... [165])
- Deleted: 9d, it shows
- Deleted: its
- Formatted (... [169])
- Formatted (... [170])
- Deleted: which verifies the variability due to wind (... [171])
- Deleted: the V2.0 SSS product,
- Formatted (... [172])
- Deleted: spatial
- Formatted (... [173])
- Formatted (... [174])
- Deleted: is found to show a different distribution in
- Deleted: 9b
- Deleted: 9e in comparison to that in Exp0. An
- Deleted: in
- Deleted: is noted outside the BS, north of Canad (... [179])
- Formatted (... [175])
- Formatted (... [176])
- Formatted (... [177])
- Formatted (... [178])
- Formatted (... [180])
- Deleted: near
- Deleted: coast in
- Deleted: (LS). It indicates that the SSS assimilati (... [183])
- Formatted (... [181])
- Formatted (... [182])
- Formatted (... [184])
- Deleted: on the shelf region of ESS is higher cor (... [185])
- Formatted (... [186])
- Deleted: , but lower near the southwest coast of LS.
- Formatted (... [150])
- Formatted (... [151])
- Formatted (... [152])

1448 [negative anomaly related to an incorrect location of the model river runoff, corrected in later](#)
 1449 [versions of the model. The SSS assimilation is able to correct the related fresh bias. In the](#)
 1450 [central Arctic, although the assimilated SSS measurements are masked by the sea ice](#)
 1451 [cover, the FWC differences north of 84°N are more pronounced in October than in](#)
 1452 [September, which indicates the advection of SSS increments by the Transpolar Drift Stream](#)
 1453 [\(Rigor et al., 2002; Balibrea-Iniesta et al., 2018\).](#) These results suggest that the SSS
 1454 assimilation of both versions of [SMOS](#) satellite products will [compensate for the insufficient](#)
 1455 [river summer runoff](#), redistribute the freshwater in the Arctic, and [adjust](#) the freshwater
 1456 budget. However, [because of](#) the limited [in-situ data](#), [the above assessment remains](#)
 1457 [qualitative](#).
 1458 Further, we [compare](#) the daily time series of [Arctic-averaged FWC](#) from the three runs [to the](#)
 1459 north of 70°N (Fig. [11](#)). The [FWC increases in](#) October-November to reach [its](#) maximum, and
 1460 gradually decreases thereafter. The impact of weekly data assimilation cycles is visible as
 1461 instantaneous jumps on the three curves of the time series, [but the assimilation of SSS does](#)
 1462 [not cause unrealistic imbalances](#). The [FWC increases](#) substantially due to SSS [assimilation](#),
 1463 [by about 25 cm](#). Notably, the assimilation of version 3.1 SSS [causes a](#) faster increase during
 1464 the first two months. [Due to the absence of](#) ground truth data in 2016, the above comparison
 1465 [remains](#) qualitative, but the timing [of the peak](#) is in better agreement with the ITP data
 1466 presented by Rosenblum et al. (2021, their Fig. 4), although the amplitude of the seasonal
 1467 FWC seems too small in all experiments, which can be related to insufficient thick ice in
 1468 [TOPAZ](#) (Uotila et al., 2019). More concrete evidence about the changed FWC will be
 1469 provided [when the longer assimilation of the satellite-based SSS product is finished in the](#)
 1470 near future.

1471

1472 5. Summary and discussions.

1473 [The gridded SSS products](#) from [the](#) SMOS [satellite](#) undoubtedly provide a way [to constrain](#)
 1474 [errors in salinity](#), especially for [an ocean reanalysis system](#). [The present study is the first](#)
 1475 [observing system simulation experiment](#) for [the](#) assimilation of SMOS SSS in the Arctic. In
 1476 this study, based on the [TOPAZ reanalysis system](#), [we compared the reanalysis assimilating](#)
 1477 [conventional observations with and without the](#) assimilation [of two successive](#) SMOS SSS
 1478 products [from BEC](#).
 1479 [After comparison with](#) independent SSS observations from CTD and surface water samples
 1480 along the [cruises](#), [the near-surface salinity errors](#) have been significantly reduced [compared](#)
 1481 to [the control experiment](#) (Exp0). In the Beaufort Sea, the SSS bias and RMSD in ExpV3 [are](#)
 1482 reduced respectively by 26.0% and 20.6%. [In](#) ExpV2, the RMSD [reduction](#) is [smaller](#) (by

Formatted ... [188]

Deleted: will be adjusted in the end.

Deleted: so far with

Deleted: amount of in-situ data, it is not fair to conclude whether this is a change for the better or the worse. Significantly different from sparse in-situ observations in the Arctic, the reanalysis product can better represent the characteristics of FWC variations in space and time.

Formatted: Font: (Asian) SimSun, Font colour: Auto

Formatted: Font: (Asian) SimSun, Font colour: Auto

Formatted: Font: (Asian) SimSun, 11 pt, Font colour: Auto

Deleted: intercompare... ompare the daily time series of FWCL...rctic-averaged FWC from the three runs averaged over ... [189]

Deleted: 10...1). The averaged FWCL clearly shows a sharp increase till...WC increases in October-November to reach the...ts maximum, and gradually decreases thereafter. The impact of weekly data assimilation cycles is visible as instantaneous jumps on the three curves of the time series.... but the assimilation ... [190]

Formatted: Font: (Default) Arial, (Asian) SimSun, 12 pt

Formatted ... [191]

Deleted: SSS plays a key role to track the water ... [192]

Formatted: Font: (Asian) SimSun, Font colour: Auto

Deleted: . ExpV2 and ExpV3 additionally assimil... [193]

Formatted: Font: (Asian) SimSun, Font colour: Auto

Deleted: , which were tested and retrieved by a ... [194]

Formatted: Font: (Asian) SimSun, Font colour: Auto

Deleted: Evaluated by the

Formatted: Font: (Asian) SimSun, Font colour: Auto

Deleted: cruise underway, the quantitative misfit... [195]

Deleted: relative

Formatted: Font: (Asian) SimSun, Font colour: Auto

Formatted: Font: (Asian) SimSun, Font colour: Auto

Deleted: that in

Deleted: .

Deleted: is

Formatted: Font: (Asian) SimSun, Font colour: Auto

Formatted: Font: (Asian) SimSun, Font colour: Auto

Formatted: Font: (Asian) SimSun, Font colour: Auto

Deleted: %, and if validated only against the ... [196]

Deleted: reduced

Formatted ... [197]

Formatted: Font: (Asian) SimSun, Font colour: Auto

Formatted: Default Paragraph Font, Font colour: Black

Formatted: Default Paragraph Font, Font colour: Black

Formatted ... [187]

1622 11.5%). In the Chukchi Sea, the reduction in SSS misfits in ExpV3 (bias:17.7%; RMSD:
1623 16.4%) is also larger than in ExpV2 (bias: 15.5%; RMSD: 13.7%). Around Greenland, the
1624 difference between the two products is even more pronounced, with a significant reduction in
1625 the SSS bias (32.6%) and RMSD (9.4%) in ExpV3, while there is no notable improvement in
1626 ExpV2. The difference is larger in the East Greenland Sea. The direct assimilation of SSS
1627 from SMOS is more efficient at constraining the near-surface salinity than the multivariate
1628 impact of other observations. This finding is also consistent with other SSS assimilation
1629 experiments in the tropics (Chakraborty et al., 2015; Tranchant et al., 2019). Conversely,
1630 when considering the multivariate impact of SSS on SIC (in Fig. 9) we find that the
1631 assimilation of the V2 product does not affect the assimilation of sea ice concentrations while
1632 the V3.1 product causes an increase in the negative increments, which could be an
1633 indication of excessive freshening along the Siberian coasts. In contrast, the increments of
1634 SST in the open ocean are smaller in ExpV3, indicating a synergy effect of SST and SSS.
1635 Overall, our data assimilation system did not detect obvious inconsistencies between the
1636 SMOS SSS product and other assimilated observations.

1638 Furthermore, this study shows error reductions of SSS when assimilating the V3.1 product
1639 from SMOS, even outside of the central Arctic, in the Nordic Seas and along the Norwegian
1640 coast. Moreover, our analysis shows how the spatial distribution of Arctic FWC changes as a
1641 result of assimilating the two SMOS products. The time series of averaged FWC north of
1642 70°N shows that the FWC in the whole central Arctic can be increased by about 25 cm using
1643 DA. Our experiments show that the Arctic FWC can be redistributed horizontally after
1644 assimilation, but the latter effect requires a longer assimilation run to be evaluated.
1645 As a summary of the quantitative SSS comparisons (Table 2), the overall score of each
1646 assimilation setup for each subregion can be defined by its ability to reduce the SSS bias
1647 and RMSD by more than 9% relative to Exp0 (Fig. 2). If both bias and RMSD meet the
1648 objective, we give a score of 1, but of 2 if only one of them is met. If neither of them exceeds
1649 9%, the score is set to 3. Thus outside of the central Arctic, the v2.0 SSS product loses its
1650 impact on the TOPAZ system, but the V3.1 SSS brings significant impacts across the Arctic,
1651 and further out, and clearly benefits from its refined effective resolution (Martínez et al.,
1652 2022). Since there was little evidence of a double-penalty effect in the validation RMSD apart
1653 from Baffin Bay, we consider that the assimilation of the higher resolution signals was
1654 efficient. However, the assimilation did not improve the SSS significantly in the Barents Sea
1655 or other areas where SSS gradients are weak. These may require higher accuracy to
1656 distinguish the Atlantic waters from other water masses of salinity only slightly below 35 psu.
1657 To further improve the SSS product, a combination with the Aquarius sensor using the same

Deleted: % (if validated against the BGEP CTD profiles about 10.5% in Fig. 4).

Formatted: Font: (Asian) SimSun, Font colour: Auto

Deleted: more

Deleted: that

Deleted: validated by the SSS observations from OMG,

Formatted: Font: (Asian) SimSun, Font colour: Auto

Formatted: Font: (Asian) SimSun, Font colour: Auto

Formatted: Font: (Asian) SimSun, Font colour: Auto

Deleted: is found

Formatted: Font: (Asian) SimSun, Font colour: Auto

Deleted: Furthermore, dividing the observations around Greenland into two regions, S5 and S6 (Table 2 and Fig. 7) show a larger reduction in the bias (52%) and RMSD (10.5%) in the Greenland Sea (S5) in ExpV3 SSS relative to that in Exp0. Notably in the Baffin Bay (S6), only the SSS bias in ExpV3 shows an obvious reduction compared with Exp0. It is

Deleted: the markable adjustment along the 34 psu isoline near the ice edge in GS (shown in Fig. 3). Increments of SSS (in Fig. 8) also clearly show the wide salty features located in the GS in ExpV3, which is clearly different to that in Exp0 and ExpV2. In addition, the increments for other variables such as SST, SIC and so on are diagnosed, but their spatial features during the same time (figures not shown) have no clear differences as in Exp0. It further verifies the surface salinity is dominantly constrained by the direct observations from SMOS, other than the weak constraints through the error covariance from other observed variables. This finding also is consistent with the conclusions in

Formatted: Font: (Asian) SimSun, Font colour: Auto

Formatted: Font: (Asian) SimSun, Font colour: Auto

Deleted: 2015; Tranchant et al., 2019).

Deleted: that the error reduction...eductions of SSS will be benefited from the assimilation of...hen assimilating the V3.1 product from SMOS,...even outside of the central Arctic. A remarkable improvement is also achieved around GS (S5 in Fig. 1), a clear advantage compared to the other version of SSS product...in the Nordic Seas and along the Norwegian coast. Moreover, our analysis shows different...ow the spatial

Deleted: corrected by the SSS innovations though ...increased by about 25 cm using DA, al...

Formatted: Font: (Default) Arial, (Asian) SimSun, 12 pt

Deleted: ¶

Deleted: 9-days SSS. In fact, the V3.1 SSS also provides a 3-days product that needs to be teste...

Formatted: Font: (Asian) SimSun, English (US)

Formatted: Default Paragraph Font, Font colour: Black

Formatted: Default Paragraph Font, Font colour: Black

Formatted

Formatted

Formatted

1860 L-band frequency (e.g., Lee et al, 2012), and SMAP (e.g., Tang et al., 2017; Reul et al.,
1861 [2020](#)) is desirable.

1863 **Data availability.** All the in-situ observations for validation in this study are open access, as
1864 indicated in Sect. 3. The model results from Exp0 are the released TOPAZ reanalysis, which
1865 is freely available from CMEMS (<http://marine.copernicus.eu>) or
1866 <https://doi.org/10.11582/2022.00043>. The other assimilation experiments can be provided
1867 freely upon personal communication.

1869 **Author contributions.** JX initiated the design and carried out the assimilation
1870 experiments. LB and RR contributed to the result interpretation. JM provided the SSS data.
1871 CG and RC contributed to the uncertainty of the satellite data. All the authors contributed to
1872 editing and correcting this paper.

1874 **Competing interests.** The authors declare that they have no conflict of interest.

1876 Acknowledgments:

1877 We are grateful to the in-situ data providers: the OMG mission for the released final CTD
1878 data via <https://podaac.jpl.nasa.gov/omg>; the ICES data portal (<https://www.ices.dk>); the
1879 Arctic Data Center (<https://arcticdata.io/catalog/data>); and the BGEP data were available at
1880 the Woods Hole Oceanographic Institution (<https://www2.whoi.edu/site/beaufortgyre/>) in
1881 collaboration with researchers from Fisheries and Oceans Canada at the Institute of Ocean
1882 Sciences. This study has been supported by the ESA Arctic+Salinity project and the
1883 following CCN, and also partly by the Norwegian Research Council project (325242). The
1884 assimilation experiments and the plotting of the results were performed on resources
1885 provided by Sigma2, the Norwegian Infrastructure for High Performance Computing and
1886 Data Storage with the projects nn2293k and nn9481k and the storage areas under the
1887 projects ns9481k and ns2993k.

1889 Reference:

- Deleted: Aquarius used three radiometers at fixe... [206]
- Deleted: had a 350 km wide swath that covered ... [208]
- Deleted: scans earth using a spinning antenna, V... [210]
- Formatted ... [207]
- Formatted ... [209]
- Formatted ... [211]
- Deleted: 2020). To combine all the SSS retrieve... [212]
- Formatted ... [213]
- Deleted:
- Deleted: accessed
- Formatted ... [214]
- Formatted ... [216]
- Formatted ... [217]
- Formatted ... [218]
- Formatted ... [215]
- Deleted: the states
- Deleted: result in
- Deleted: same as
- Deleted: from TOPAZ4
- Formatted ... [219]
- Formatted ... [220]
- Formatted ... [221]
- Formatted ... [222]
- Deleted: ...u). Other two ... [223]
- Deleted: data
- Formatted ... [224]
- Formatted ... [225]
- Deleted: freely
- Formatted ... [226]
- Deleted: for public by
- Formatted ... [227]
- Formatted ... [228]
- Deleted: carry of
- Formatted ... [229]
- Formatted ... [230]
- Deleted: JC collected
- Formatted ... [231]
- Deleted: enhanced the understanding for
- Deleted: contribute
- Formatted ... [232]
- Formatted ... [233]
- Deleted: edit
- Formatted ... [234]
- Deleted: correct
- Formatted ... [235]
- Deleted: Competinginterests
- Formatted ... [236]
- Formatted ... [237]
- Deleted: Thanks...e are grateful to the profile...r... [238]
- Formatted ... [239]
- Deleted: based
- Formatted ... [240]
- Deleted:
- Deleted: +
- Formatted ... [241]
- Formatted ... [242]
- Deleted: NFR Thickness of Arctic sea ice Recon... [243]
- Formatted ... [244]
- Deleted: .
- Deleted: computation of the...assimilation exper... [246]
- Formatted ... [245]
- Formatted ... [247]
- Formatted ... [248]
- Formatted ... [203]

1995 [Balibrea-Iñiesta, F., Xie, J., Garcia-Garrido, V., Bertino, L., Maria Mancho, A., and Wiggins, S.: Lagrangian transport across the upper Arctic waters in the Canadian Basin. Q. J. Roy. Meteor. Soc., 145\(718\), 76-91, doi:10.1002/qj.3404, 2018.](#)

1996

1997

1998 [Bertino, L., Ali, A., Carrasco, A., Lien, V., and Melsom, A.: THE ARCTIC MARINE FORECASTING CENTER IN THE FIRST COPERNICUS PERIOD. 9th EuroGOOS International conference, Shom: Ifremer: EuroGOOS AISBL, May 2021, Brest, France. pp.256-263. hal-03334274v2. \(Available from <https://hal.archives-ouvertes.fr/hal-03334274v2/document>\)](#)

1999

2000

2001

2002 Bouillon, S., Fichetef, T., Legat, V., and Madec, G.: The elastic-viscous-plastic method revised, Ocean Modell., 7, 2–12, doi:10.1016/j.ocemod.2013.05.013, 2013.

2003

2004 [Boutin, J., Jean-Luc, V., and Dmitry, K.: SMOS SSS L3 maps generated by CATDS CEC LOCEAN, debias V3.0. SEANOE. 2018. Available online: <https://www.seanoe.org/data/00417/52804/>.](#)

2005

2006

2007 [Boutin J., Vergely J.-L., and Khvorostyanov D.: SMOS SSS L3 maps generated by CATDS CEC LOCEAN. debias V7.0. SEANOE. doi:10.17882/52804#91742, 2022.](#)

2008

2009 Boyer, T. P., Levitus, S., Antonov, J. I., Locarnini, R. A., and Garcia, H. E.: Linear trends in salinity for the World Ocean, 1955–1998, Geophys. Res. Lett., 32, L01604, doi:10.1029/2004GL021791, 2005.

2010

2011

2012 [Carmack, E. C., Yamamoto Kawai, M., Haine, T. W. N., Bacon, S., Bluhm, B. A., Lique, C., Melling, H., Polyakov, I. V., Straneo, F., Timmermans, M.-L., and Williams, W. J.: Freshwater and its role in the Arctic Marine System: Sources, disposition, storage, export, and physical and biogeochemical consequences in the Arctic and global oceans, J. Geophys. Res. Biogeo., 121, 675–717, doi:10.1002/2015JG003140, 2016.](#)

2013

2014

2015

2016

2017 [Chakraborty, A., Sharma, R., Kumar, R., and Basu, S.: Joint Assimilation of Aquarius-derived Sea Surface Salinity and AVHRR-derived Sea Surface Temperature in an Ocean General Circulation Model Using SEEK Filter: Implication for Mixed Layer Depth and Barrier Layer Thickness, J. Geophys. Res. Oceans, 120 \(10\), 6927-6942, doi:10.1002/2015JC010934, 2015.](#)

2018

2019

2020

2021

2022 [Chassignet, E. P., Smith, L. T., and Halliwell, G. R.: North Atlantic Simulations with the Hybrid Coordinate Ocean Model \(HYCOM\): Impact of the vertical coordinate choice, reference pressure, and thermobaricity, J. Phys. Oceanogr., 33, 2504–2526, doi:10.1175/1520-0485\(2003\)033<2504:NASWTH>2.0.CO;2, 2003.](#)

2023

2024

2025

2026 [Cooper, L. W., Grebmeier, J. M., Frey, K. E., and Vaglem, S.: Discrete water samples collected from the Conductivity-Temperature-Depth rosette at specific depths, Northern Bering Sea to Chukchi Sea, 2016. Arctic Data Center. doi:10.18739/A23B5W875, 2019.](#)

2027

2028

2029 [Curry, R., Dickson, R., and Yashayaev, I.: A change in the freshwater balance of the Atlantic Ocean over the past four decades, Nature, 426, 826–829, doi:10.1038/nature02206, 2003.](#)

2030

Deleted: https://

Deleted: .org/

Formatted: Font: (Asian) SimSun, Font colour: Auto

Deleted: https://doi.org/10.17882/52804#91742

Formatted: Font: Times New Roman, 12 pt

Deleted: f

Deleted: .-

Deleted: https://

Deleted: .org/

Formatted: Font: (Asian) SimSun, Font colour: Black

Deleted: .-

Deleted:

Formatted: Font: (Asian) SimSun, Font colour: Black

Formatted: Font: (Asian) SimSun, Font colour: Black

Formatted: Font: Times New Roman, 12 pt

Formatted: Font: Times New Roman, 12 pt

Field Code Changed

Formatted: Font: Times New Roman, 12 pt

Formatted: Default Paragraph Font, Font colour: Black

Formatted: Default Paragraph Font, Font colour: Black

Formatted: Normal, Right: 0,63 cm, Border: Top: (No border), Bottom: (No border), Left: (No border), Right: (No border), Between : (No border), Tab stops: 7,96 cm, Centred + 15,92 cm, Right, Position: Horizontal: Left, Relative to: Column, Vertical: In line, Relative to: Margin, Wrap Around

2040 Dombrowsky, E., Bertino, L., Cummings, J., Brassington, G. B., Chassignet, E. P., Davidson,
 2041 F., [Hurlburt, H. E., Kamachi, M., Lee, T., Martin, M. J., Mei, S., and Tonani, M.](#): GODAE
 2042 systems in operations. *Oceanography*, 22(3), 80–95, [doi:10.5670/oceanog.2009.68](https://doi.org/10.5670/oceanog.2009.68), 2009
 2043 Drange, H. and Simonsen, K.: Formulation of air-sea fluxes in the ESOP2 version of MICOM,
 2044 Technical Report No. 125, Nansen Environmental and Remote Sensing Center, 23 pp.,
 2045 1996.

2046 [Fenty, I., Willis, J. K., Khazendar, A., Dinardo, S., Forsberg, R., Fukumori, I., Holland, D.,](#)
 2047 [Jakobsson, M., Moller, D., Morison, J., Meuncho, A., Rignot, E., Schodlock, M.,](#)
 2048 [Thompson, A.F., Tino, K., Rutherford, M., and Trenholm, N.](#): Oceans Melting Greenland:
 2049 Early results from NASA's ocean-ice mission in Greenland. *Oceanography*, 29(4):72-83,
 2050 [doi:10.5670/oceanog.2016.100](https://doi.org/10.5670/oceanog.2016.100), 2016.

2051 Font, J., Camps, A., Borges, A., Martín-Neira, M., Boutin, J., Reul, N., Kerr, Y. H., Hahne, A.,
 2052 and Mecklenburg, S.: SMOS: The challenging sea surface salinity measurement from
 2053 space, *Proc. IEEE*, 98(5), 649–665, [doi:10.1109/JPROC.2009.2033096](https://doi.org/10.1109/JPROC.2009.2033096), 2010,
 2054 [Fournier, S., Lee, T., Wang, X., Armitage, T. W. K., Wang, O., Fukumori, I., and Kwok, R.:](#)
 2055 [Sea Surface Salinity as a Proxy for Arctic Ocean Freshwater Changes.](#) *Journal of*
 2056 [Geophysical Research: Oceans](#), 125(7). [doi:10.1029/2020JC016110](https://doi.org/10.1029/2020JC016110), 2020

2057 Fujii, Y., Rémy, E., Zuo, H., Oke, P., Halliwell, G., Gasparin, F., et al.: Observing system
 2058 evaluation based on ocean data assimilation and prediction systems: on-going challenges
 2059 and a future vision for designing and supporting ocean observational networks. *Front. Mar.*
 2060 *Sci.*, 6(417), [doi:10.3389/fmars.2019.00417](https://doi.org/10.3389/fmars.2019.00417), 2019.

2061 Goñi, M. A., Corvi, E. R., Welch, K. A., Buktenica, M., Lebon, K., Alleau, Y., and Juranek, L.
 2062 W.: Particulate organic matter distributions in surface waters of the Pacific Arctic shelf
 2063 during the late summer and fall season. *Marine Chemistry*, 211, 75-93,
 2064 [doi:10.1016/j.marchem.2019.03.010](https://doi.org/10.1016/j.marchem.2019.03.010), 2019.

2065 Goñi, M. A., Juranek, L. W., Sipler, R. E., and Welch, K. A.: Particulate organic matter
 2066 distributions in the water column of the Chukchi Sea during late summer. *J. Geophys. Res.*,
 2067 *Oceans*, 126(9), [doi:10.1029/2021JC017664](https://doi.org/10.1029/2021JC017664), 2021.

2068 [Greiner, E., Verbrugge, N., Mulet, S., and Guinehut, S.:](#) [Quality information document for multi](#)
 2069 [observation global ocean 3D temperature salinity heights geostrophic currents and MLD](#)
 2070 [product.](#) [CMEMS-MOB-QUID-015-012.](#) [available](#) [at:](#)
 2071 [https://catalogue.marine.copernicus.eu/documents/QUID/CMEMS-MOB-QUID-015-](https://catalogue.marine.copernicus.eu/documents/QUID/CMEMS-MOB-QUID-015-012.pdf)
 2072 [012.pdf](#) (last access: 14 December 2022), 2021.

2073 Janout, M. A., [Hölemann, J., Timokhov, I., Gutjahr, O., and Heinemann, G.:](#) Circulation in the
 2074 northwest Laptev Sea in the eastern Arctic Ocean: Crossroads between Siberian River

Deleted: ...

Deleted: . (2009).

Formatted: Font: (Asian) SimSun, Font colour: Auto

Deleted: . <https://doi.org/10.5670/oceanog.2009.68>

Deleted: Evensen, G.: The ensemble Kalman filter: theoretical formulation and practical implementation, *Ocean Dynam.*, 53, 343–367, [doi:10.1007/s10236-003-0036-9](https://doi.org/10.1007/s10236-003-0036-9), 2003

Deleted: <https://doi.org/10.5670/ocean.2016.100>

Formatted: Indent: Left: 0 cm, Hanging: 0.5 cm, Border: Top: (No border), Bottom: (No border), Left: (No border), Right: (No border), Between: (No border)

Deleted: DOI: [10.1109/JPROC.2009.2033096](https://doi.org/10.1109/JPROC.2009.2033096)

Formatted: Font: (Asian) SimSun, Font colour: Auto, Not Highlight

Deleted: .

Deleted: .

Deleted: .

Deleted: .

Formatted: Font: (Asian) SimSun, Font colour: Auto, Not Highlight

Deleted: *Journal of Geophysical Research:*

Formatted: Font: (Asian) SimSun, Font colour: Custom Colour (RGB(44,44,44))

Deleted: . Hölemann, L.

Deleted: O.

Deleted: G.

Deleted: .

Formatted: Font: (Asian) SimSun, Font colour: Auto

Formatted: Default Paragraph Font, Font colour: Black

Formatted: Default Paragraph Font, Font colour: Black

Formatted: Normal, Right: 0,63 cm, Border: Top: (No border), Bottom: (No border), Left: (No border), Right: (No border), Between: (No border), Tab stops: 7,96 cm, Centred + 15,92 cm, Right, Position: Horizontal: Left, Relative to: Column, Vertical: In line, Relative to: Margin, Wrap Around

2094 water, Atlantic water and polynya-formed dense water, *J. Geophys. Res. Oceans*, 122,
2095 6630–6647, doi:10.1002/2017JC013159, 2017.

2096 Johannessen, O. M., Shalina, E. V., and Miles, M. W.: Satellite [evidence](#) for an Arctic Sea ice
2097 cover in transformation, *Science*, 286, 1937–1939, doi:10.1126/science.286.5446.1937,
2098 1999.

2099 [Kaminski, T., Kauker, F., Eicken, H., and Karcher, M.: Exploring the utility of quantitative
2100 network design in evaluating Arctic sea ice thickness sampling strategies. *The Cryosphere*,
2101 9\(4\), 1721–1733, doi:10.5194/tc-9-1721-2015, 2015](#)

2102 Kerr, Y. H., Waldteufel, P., Wigneron, J. P., Delwart, S., Cabot, F., Boutin, J., Escorihuela, M.
2103 J., Font, J., Reul, N., Gruhier, C., Juglea, S., Drinkwater, M. R., Hahne, A., Martín-Neira,
2104 M., and Mecklenburg, S.: The SMOS mission: New tool for monitoring key elements of the
2105 global water cycle, *Proc. IEEE*, 98(5), 666–687, doi:10.1109/JPROC.2010.2043032, 2010.

2106 Lee, T., Lagerloef, G., Gierach, M. M., Kao, H. -Y., Yueh, S. S., and Dohan, K.: Aquarius
2107 reveals salinity structure of tropical instability waves. *Geophys. Res. Lett.*, 39, L12610,
2108 doi:10.1029/2012GL052232, 2012.

2109 [Lisæter, K. A., Rosanova, J. and Evensen, G.: Assimilation of ice concentration in a coupled
2110 ice-ocean model, using the Ensemble Kalman filter, *Ocean Dyn.*, 53\(4\), 368–388,
2111 doi:10.1007/s10236-003-0049-4, 2003.](#)

2112 Lu, Z., Cheng, L., Zhu, J., and Lin, R.: The complementary role of SMOS sea surface salinity
2113 observations for estimating global ocean salinity state, *J. Geophys. Res. Oceans*, 121,
2114 doi:10.1002/2015JC011480, 2016.

2115 [Martin, M. J., King, R. R., While, J., Aguiar, A. B.: Assimilating satellite sea-surface salinity
2116 data from SMOS, Aquarius and SMAP into a global ocean forecasting system. *Q. J. Roy.
2117 Meteor. Soc.*, 145\(719\), 705-726, doi:10.1002/qj.3461, 2019.](#)

2118 Martínez, J., Gabarró, C., and Turiel, A.: Algorithm Theoretical Basis Document, Arctic+Salinity
2119 ITT, Tech. rep., BEC, Institut de Ciències del Mar-CSIC,
2120 doi:10.13140/RG.2.2.12195.58401, 2020.

2121 Martínez, J., Gabarró, C., Turiel, A., González-Gambau, V., Umbert, M., Hoareau, N.,
2122 González-Haro, C., Olmedo, E., Arias, M., Catany, R., Bertino, L., Raj, R. P., Xie, J., Sabia,
2123 R., and Fernández, D.: Improved BEC SMOS Arctic Sea Surface Salinity product v3.1,
2124 *Earth Syst. Sci. Data*, 14, 307–323, doi:10.5194/essd-14-307-2022, 2022.

2125 [Martín-Neira, M., Oliva, R., Corbella, I., Torres, F., Duffo, N., Durán, I., Kainulainen, J., Closa,
2126 J., Zurita, A., Cabot, F., Khazaal, A., Anterrieu, E., Barbosa, J., Lopes, G., Tenerelli, J.,
2127 Díez-García, R., Fauste, J., Martín-Portuerras, F., González-Gambau, V., Turiel, A.,
2128 Delwart, S., Crapolicchio, R., and Suess, M.: SMOS instrument performance and calibration
2129 after six years in orbit. *Remote Sens. Environ.*, 180, doi:10.1016/j.rse.2016.02.036, 2016.](#)

Deleted: ev- idence

Deleted: https://

Deleted: .org/

Formatted: Font: (Asian) SimSun, Italic

Deleted: &

Deleted: . (2015).

Formatted: Font: (Asian) SimSun, Font colour: Black,

Formatted: Font: (Asian) SimSun, Font colour: Black,

Formatted: Font: (Asian) SimSun, Font colour: Black,

Formatted: Font: (Asian) SimSun, Font colour: Black

Formatted: Font: (Asian) SimSun, Italic, Font colour: Black

Formatted: Font: (Asian) SimSun, Font colour: Black

Deleted: .

Deleted: https://doi.org/10.5194/tc-9-1721-2015

Formatted: Font: (Asian) SimSun, Font colour: Black

Formatted: Font: (Asian) SimSun, Font colour: Black

Deleted: Lv, S., Schalge, B., Saavedra Garfias, P., and Simmer, C.: Required sampling density of ground-based soil moisture and brightness temperature observations for calibration and validation of L-band satellite observations based on a virtual reality, *Hydrol. Earth Syst. Sci.*, 24, 1957–1973, https://doi.org/10.5194/hess-24-1957-2020, 2020.

Deleted: Quarterly Journal of the Royal Meteorological Society,...

Formatted: Font: (Asian) SimSun, Font colour: Auto

Deleted: https://

Deleted: .org/

Deleted: https://

Deleted: .org/

Formatted: Font: (Asian) SimSun, Font colour: Black

Formatted: Default Paragraph Font, Font colour: Black

Formatted: Default Paragraph Font, Font colour: Black

Formatted: Normal, Right: 0,63 cm, Border: Top: (No border), Bottom: (No border), Left: (No border), Right: (No border), Between : (No border), Tab stops: 7,96 cm, Centred + 15,92 cm, Right, Position: Horizontal: Left, Relative to: Column, Vertical: In line, Relative to: Margin, Wrap Around

2150 [Mecklenburg, S., Drusch, M., Kerr, Y. H., Font, J., Martiín-Neira, M., Delwart, S., Buenadicha,](#)
2151 [G., Reul, N., Daganzo-Eusebio, E., Oliva, R., and Crapolicchio, R.: ESA's soil moisture and](#)
2152 [ocean salinity mission: Mission performance and operations, *IEEE TGARS*, 50, 1354–1366,](#)
2153 [doi:10.1109/TGRS.2012.2187666, 2012.](#)

2154 Olmedo, E., Martínez, J., Turiel, A., Ballabrera-Poy, J., and [Portabella, M.](#): Debaised non-
2155 Bayesian retrieval: A novel approach to SMOS Sea Surface Salinity, *Remote Sens.*
2156 *Environ.*, 193, 103–126, doi:10.1016/j.rse.2017.02.023, 2017.

2157 Olmedo, E., Gabarró, C., González-Gambau, V., Martínez, J., Ballabrera-Poy, J., Turiel, A.,
2158 Portabella, M., Fournier, S., and Lee, T.: Seven Years of SMOS Sea Surface Salinity at
2159 High Latitudes: Variability in Arctic and Sub-Arctic Regions. *Remote Sensing*. 2018;
2160 10(11):1772, doi:10.3390/rs10111772, 2018.

2161 Proshutinsky, A., Krishfield, Timmermans, M.-L., Toole, J., Carmack, E., Mclaughlin, F.,
2162 Williams, W. J., Zimmermann, S., Itoh, M., and Shimada, K.: Beaufort Gyre freshwater
2163 reservoir: State and variability from observations, *J. Geophys. Res. Oceans*, 114, 1–25,
2164 doi:10.1029/2008JC005104, 2009.

2165 Proshutinsky, A., Krishfield, R., and Timmermans, M.-L.: Introduction to special collection on
2166 arctic ocean modeling and observational synthesis (FAMOS) 2: beaufort gyre phenomenon.
2167 *J. Geophys. Res. Oceans*, 125, e2019JC015400, doi:10.1029/2019JC015400, 2020.

2168 Reul, N., Grodsky, S., Arias, M., Boutin, J., Catany, R., Chapron, B., D'Amico, F., Dinnat, E.,
2169 Donlon, C., Fore, A., Fournier, S., Guimbard, S., Hasson, A., Kolodziejczyk, N., Lagerloef,
2170 G., Lee, T., Le Vine, D., Lindstrom, E., Maes, C., Mecklenburg, S., Meissner, T., Olmedo,
2171 E., Sabia, R., Tenerelli, J., Thouvenin-Masson, C., Turiel, A., Vergely, J., Vinogradova, N.,
2172 Wentz, F., and Yueh, S.: Sea surface salinity estimates from spaceborne L-band
2173 radiometers: An overview of the first decade of [observation](#) (2010–2019), *Remote Sens.*
2174 *Environ.*, 242, 111769, doi:10.1016/j.rse.2020.111769, 2020.

2175 [Rigor, I. G., Wallace, J. M., and Colony, R. L.: Response of Sea Ice to the Arctic Oscillation,](#)
2176 [J. Climate](#), 15, 2648, doi:10.1175/1520-0442(2002)015<2648:ROSITT>2.0.CO;2, 2002.

2177 Rosenblum, E., Fajber, R., Stroeve, J. C., Gille, S. T., Tremblay, L. B., [and](#) Carmack, E. C.:
2178 Surface salinity under transitioning ice cover in the Canada Basin: Climate model biases
2179 linked to vertical distribution of [freshwater](#). *Geophysical Research Letters*, 48,
2180 e2021GL094739, doi:10.1029/2021GL094739, 2021

2181 Sakov, P., Counillon, F., Bertino, L., Lisæter, K. A., Oke, P. R., and Korablev, A.: TOPAZ4: an
2182 ocean-sea ice data assimilation [system](#) for the North Atlantic and Arctic, *Ocean Sci.*, 8,
2183 633–656, doi:10.5194/os-8-633-2012, 2012.

Deleted: Porta- bella

Deleted:

Deleted: https://

Deleted: .org/

Deleted: <https://doi.org/>

Deleted: Journal of Geophysical Research

Formatted: Font: (Asian) SimSun, Font colour: Custom Colour (RGB(44,44,44)), Not Highlight

Deleted: -

Deleted: *Journal of Geophysical Research:*

Deleted: . https://

Deleted: .org/

Formatted: Font: (Asian) SimSun, Font colour: Custom Colour (RGB(44,44,44))

Formatted: Font: (Asian) SimSun, Not Italic

Formatted: Font: (Default) Microsoft YaHei, (Asian) SimSun

Deleted: ob- servation

Formatted: Font: (Asian) SimSun, Italic

Deleted: https://

Deleted: .org/

Deleted: &

Deleted: . (2021).

Deleted: fresh water

Deleted: . https://

Deleted: .org/10.1029/2021GL094739

Formatted: Font: (Default) Microsoft YaHei, (Asian) SimSun

Deleted: sys- tem

Deleted: https://

Deleted: .org/

Formatted: Default Paragraph Font, Font colour: Black

Formatted: Default Paragraph Font, Font colour: Black

Formatted: Normal, Right: 0,63 cm, Border: Top: (No border), Bottom: (No border), Left: (No border), Right: (No border), Between : (No border), Tab stops: 7,96 cm, Centred + 15,92 cm, Right, Position: Horizontal: Left, Relative to: Column, Vertical: In line, Relative to: Margin, Wrap Around

2205 Solomon, A., Heuzé, C., Rabe, B., Bacon, S., Bertino, L., Heimbach, P., [Jnoue, J., Iovino, D.,](#)
2206 [Mottram, R., Zhang, X., Aksenov, Y., McAdam, R., Nguyen, A., Raj, R. P., and Tang, H.:](#)
2207 Freshwater in the Arctic Ocean 2010–2019. *Ocean Sci.* 17, 1081–1102. doi:10.5194/os-
2208 17-1081-2021. 2021.

2209 Steele, M., Morley, R., and Ermold, W.: PHC: A global ocean hydrography with a high-quality
2210 Arctic Ocean, *J. Climate*, 14, 2079–2087. doi: 10.1175/1520-
2211 0442(2001)014<2079:PAGOHW>2.0.CO;2. 2001.

2212 Storto, A., Alvera-Azcárate, A., Balmaseda, M. A., Barth, A., Chevallier, M., Counillon, F.,
2213 Domingues, C. M., Drevillon, M., Drillet, Y., Forget, G., Garric, G., Haines, K., Hernandez,
2214 F., Iovino, D., Jackson, L. C., Lellouche, J.-M., Masina, S., Mayer, M., Oke, P. R., Penny, S.
2215 G., Peterson, K. A., Yang, C. and Zuo, H.: Ocean Reanalyses: Recent Advances and
2216 Unsolved Challenges. *Front. Mar. Sci.*, 6(418), doi:10.3389/fmars.2019.00418, 2019.

2217 Stroeve, J. and Notz, D.: Changing state of Arctic sea ice across all seasons, *Environ. Res.*
2218 *Lett.*, 13, 103001, <https://doi.org/10.1088/1748-9326/aade56>, 2018.

2219 Stroh, J. N., Panteleev, G., Kirillov, S., Makhotin, M., and Shakhova, N.: Sea-surface
2220 temperature and salinity product comparison against external in situ data in the Arctic
2221 Ocean. *J. Geophys. Res. Oceans*, 120, 7223–7236. doi:10.1002/2015JC011005, 2015.

2222 Supply, A., Boutin, J., Vergely, J. L., Kolodziejczyk, N., Reverdin, G., Reul, N., and Tarasenko,
2223 A.: New insights into SMOS sea surface salinity retrievals in the Arctic Ocean. *Remote*
2224 *Sensing of Environment*, 249, 112027. doi:10.1016/J.RSE.2020.112027, 2020.

2225 Tang, W., Fore, A., Yueh, S., Lee, T., Hayashi, A., Sanchez-Franks, A., Martinez, J., King, B.,
2226 and Baranowski, D.: Validating SMAP SSS with in situ measurements, *Remote Sens.*
2227 *Environ.*, 200, 326–340. doi:10.1016/j.rse.2017.08.021, 2017.

2228 Tranchant, B., Remy, E., Greiner, E., and Legalloudec, O.: Data assimilation of Soil Moisture
2229 and Ocean Salinity (SMOS) observations into the Mercator Ocean operational system:
2230 focus on the El Niño 2015 event, *Ocean Sci.*, 15, 543–563. doi:10.5194/os-15-543-2019,
2231 2019.

2232 Uotila, P., Goosse, H., Haines, K., Chevallier, M., Barthélemy, A., Bricaud, C., Carton, J.,
2233 Fučkar, N., Garric, G., Iovino, D., Kauker, F., Korhonen, M., Lien, V. S., Marnela, M.,
2234 Massonnet, F., Mignac, D., Peterson, A., Sadik, R., Shi, L., Tietsche, S., Toyoda, T., Xie,
2235 J., and Zhang, Z.: An assessment of ten ocean reanalyses in the polar regions, *Clim.*
2236 *Dynam.*, 52, 1613–1650. doi:10.1007/s00382-018-4242-z, 2019.

2237 Vinogradova, N. T., Ponte, R. M., Fukumori, I. and Wang, O.: Estimating satellite salinity errors
2238 for assimilation of Aquarius and SMOS data into climate models. *J. Geophys. Res. Oceans*,
2239 119(8), 4732–4744. doi:10.1002/2014JC009906, 2014

Deleted: ...

Formatted: Font: (Asian) SimSun, Font colour: Auto

Deleted: . (2021).

Formatted: Font: (Asian) SimSun, Font colour: Auto

Formatted: Font: (Asian) SimSun, Font colour: Auto

Deleted: -

Deleted: .

Deleted: Science,

Deleted: (4),

Deleted: . <https://doi.org/10.5194/os-17-1081-2021>

Formatted: Font: (Asian) SimSun, Font colour: Auto

Formatted: Font: (Asian) SimSun, Font colour: Auto

Formatted: Font: (Asian) SimSun, Font colour: Auto

Formatted: Font: (Asian) SimSun, Font colour: Auto

Formatted: Font: (Asian) SimSun, Font colour: Auto

Deleted: 2001.

Deleted:

Formatted: Font: (Asian) SimSun, Not Italic, Font colour: Custom Colour (RGB(44,44,44))

Deleted: .-

Deleted: <https://doi.org/>

Formatted (... [250])

Formatted (... [251])

Formatted: Font: (Asian) SimSun, Not Bold

Deleted: &

Deleted: . (2020).

Deleted: . <https://doi.org/10.1016/J.RSE.2020.112027>

Deleted: <https://>

Deleted: .org/

Deleted: <https://>

Deleted: .org/

Deleted: <https://>

Deleted: <https://>

Deleted: .org/

Formatted: Font: (Asian) SimSun, Pattern: Clear

Deleted: . (2014)

Formatted: Font: (Asian) SimSun, Font colour: Auto

Deleted: *Journal of Geophysical Research:*

Formatted (... [252])

Formatted (... [253])

Deleted: .

Deleted: <https://doi.org/>

Formatted: Default Paragraph Font, Font colour: Black

Formatted: Default Paragraph Font, Font colour: Black

Formatted (... [249])

2264 Woodgate, R. A., Weingartner, T. J., and Lindsay, R.: Observed increases in Bering Strait
 2265 oceanic fluxes [from the](#) Pacific to the Arctic from 2001 to 2011 and their impacts [on the](#)
 2266 Arctic Ocean water column. *Geophys. Res. Lett.*, 39, L24603, [doi:10.1029/2012GL054092](#),
 2267 2012.

2268 Xie, J., Bertino, L., Counillon, F., Lisæter, K. A., and Sakov, P.: Quality assessment of the
 2269 TOPAZ4 reanalysis in the Arctic over the period 1991-2013. *Ocean Science*, **13**(1). doi:
 2270 10.5194/os-13-123-2017, 2017.

2271 Xie, J., Counillon, F., and Bertino, L.: Impact of assimilating a merged sea-ice thickness from
 2272 CryoSat-2 and SMOS in the Arctic reanalysis. *The Cryosphere*, **12**(11), 3671-3691. doi:
 2273 10.5194/tc-12-3671-2018, 2018.

2274 Xie, J., Raj, R. P., Bertino, L., Samuelsen, A., and Wakamatsu, T.: Evaluation of Arctic Ocean
 2275 surface salinities from the Soil Moisture and Ocean Salinity (SMOS) mission against a
 2276 regional reanalysis and in situ data, *Ocean Sci.*, **15**, 1191–1206, [doi:10.5194/os-15-1191-](#)
 2277 2019, 2019.

2278 Yu, L.: A global relationship between the ocean water cycle and near-surface salinity, *J.*
 2279 *Geophys. Res.*, **116**, C10025, [doi:10.1029/2010JC006937](#), 2011.

2280 [Yu, L., Jin, X., Josey, S. A., Lee, T., Kumar, A., Wen, C., and Xue, Y.:](#) The Global Ocean Water
 2281 Cycle in Atmospheric Reanalysis, Satellite, and Ocean Salinity, *J. Climate*, **30**(10), 3829-
 2282 3852, [doi:10.1175/JCLI-D-16-0479.1](#), 2017

2283 Yueh, S., West, R., Wilson, W., Li, F., Nghiem, S., and Rahmat- Samii, Y.: Error Sources and
 2284 Feasibility for Microwave Remote Sensing of Ocean Surface Salinity, *IEEE T. Geosci.*
 2285 *Remote*, **39**, 1049–1059, [doi: 10.1109/36.921423](#), 2001.

2286 Zweng, M. M., Reagan, J. R., Antonov J. I., Locarnini, R. A., Mishonov, A. V., Boyer, T. P.,
 2287 Garcia, H. E., Baranova, O. K., Johnson, D. R., Seidov, D., and Biddle, M. M.: World Ocean
 2288 Atlas 2013, Volume 2: Salinity, Levitus, S. (Ed.), Mishonov, A., Technical Ed. NOAA Atlas
 2289 NESDIS 74, 39pp, [doi:10.7289/V5251G4D](#), 2013.

Deleted: fromthe
 Deleted: onthe

Deleted: https://
 Deleted: .org/

Deleted: https://
 Deleted: .org/
 Formatted: Font: (Asian) SimSun, Font colour: Black
 Deleted: Journal of
 Formatted: Font: (Asian) SimSun, Font colour: Black
 Formatted: Font: (Asian) SimSun, Font colour: Black

Deleted: 2001.

Formatted: Default Paragraph Font, Font colour: Black
 Formatted: Default Paragraph Font, Font colour: Black
 Formatted: Normal, Right: 0,63 cm, Border: Top: (No border), Bottom: (No border), Left: (No border), Right: (No border), Between : (No border), Tab stops: 7,96 cm, Centred + 15,92 cm, Right, Position: Horizontal: Left, Relative to: Column, Vertical: In line, Relative to: Margin, Wrap Around

Caption and figures:

Table 1. Settings of the three assimilation runs in 2016 with and without SSS.

	Assimilated obs.	Initial model states	End date of assimilation	SSS Observation Errors
Exp0	SST, SLA, T/S profile, SIC, SIT, and SID	6 th July	28 th Dec.	N/A
ExpV2	SSS V2.0 + obs. used in Exp0	6 th July	28 th Dec.	Eq. 3
ExpV3	SSS V3.1 + obs. used in Exp0	6 th July	28 th Dec.	Eq. 3

Table 2. Evaluation of SSS misfits (unit: psu) in the three assimilation runs according to the 6 areas indicated by the blue dashed lines in Fig. 2. The numbers in bold indicate the smallest misfit with a reduction of at least 9% relative to Exp0. The overall score depends on whether the bias and RMSD are reduced by at least 9%. If both criteria are met, the score equals 1, it is 2 if only one of them is met, and 3 otherwise. The star subscript means the bias changes passed the significance test using Student's t-test ($\alpha = 0.05$).

	Areas in Fig. 2	Number of obs.	Bias (psu)			RMSD (psu)			Overall score	
			Exp0	ExpV2	ExpV3	Exp0	ExpV2	ExpV3	ExpV2	ExpV3
	BS	98	2.8	2.43	2.08	2.8	2.54	2.28	1*	1*
	CS	137	2.3	1.96	1.91	2.6	2.26	2.19	1*	1*
	BSS	189	1.3	1.34	1.30	2.5	2.49	2.47	3	3
	NS	669	0.4	0.44	0.37	1.1	1.19	1.16	3	2
	GS	254	0.5	0.51	0.24	1.4	1.43	1.28	3	1*
	BB	89	0.3	0.37	0.12	1.2	1.20	1.22	3	2

Formatted

Deleted: sub-regions

Deleted: 1

Deleted: fonts

Deleted: minimal misfits in the runs

Deleted: significant

Deleted: (>

Deleted: with respect

Deleted:).

Deleted: is defined by

Deleted: reductions of

Deleted: significant or not.

Deleted: reductions

Deleted: significant

Deleted: index

Deleted: but

Deleted: reduced

Deleted: equals 3.

Deleted: Region

Deleted Cells

Deleted: 1

Deleted Cells

Deleted: S1

Deleted Cells

Deleted: S2

Deleted: S3

Deleted: S4

Deleted: S5

Deleted: S6

Formatted: Font colour: Black

Formatted: Normal, Right: 0.63 cm, Border: Top: (No border), Bottom: (No border), Left: (No border), Right: (No border), Between : (No border), Tab stops: 7,96 cm, Centred + 15,92 cm, Right

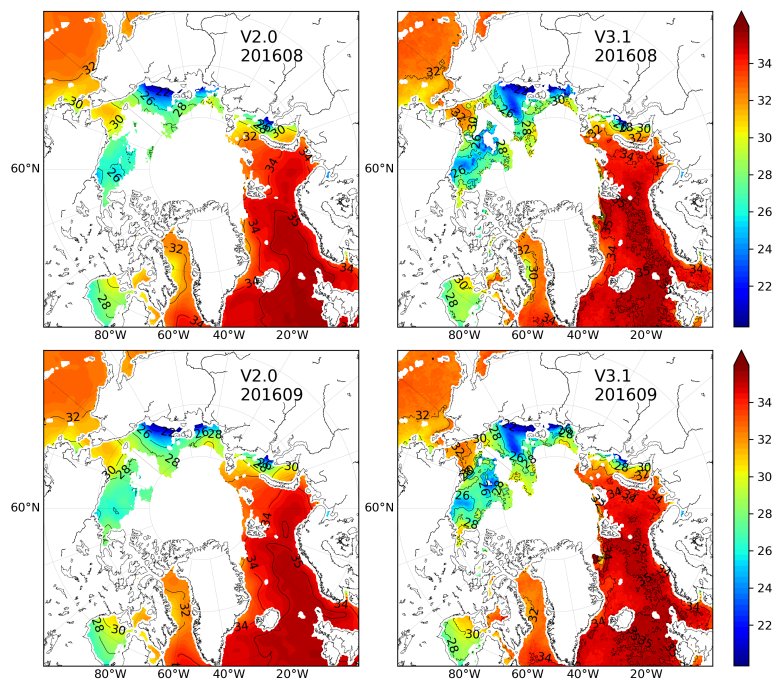


Fig. 1 Monthly SSS of Aug (top line) and Sep (bottom line) in 2016 from SMOS products of BEC V2.0 (left) and V3.1 (right). Note: the solid isolines of SSS are 22, 26, 28, 30, 32, 34, and 35 psu.

Moved (insertion) [1]
 Formatted: Font: Bold

Formatted: Font colour: Black
 Formatted: Normal, Right: 0.63 cm, Border: Top: (No border), Bottom: (No border), Left: (No border), Right: (No border), Between : (No border), Tab stops: 7,96 cm, Centred + 15,92 cm, Right

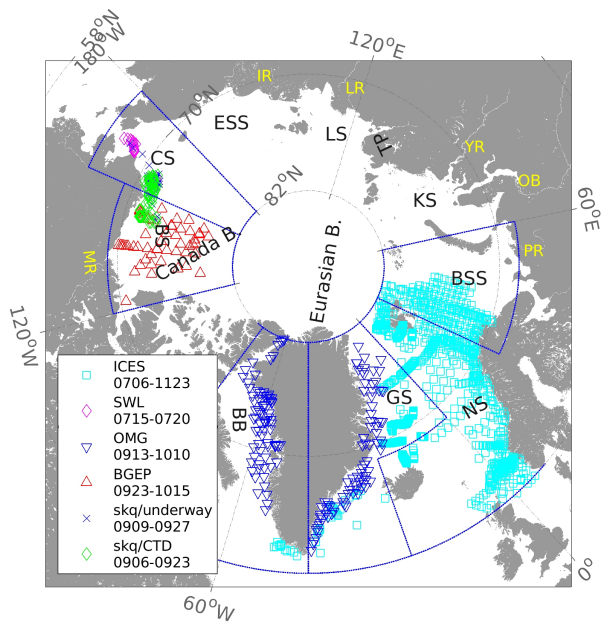


Fig. 2 Locations of the observed SSS from in-situ profiles and surface samples by cruises from July to December 2016. [The marks note](#) 6 observation sources, see the details in Section 2.3. The marginal seas delineated are the Beaufort Sea (BS), Chukchi Sea (CS), East Siberian Sea (ESS), Laptev Sea (LS), Kara Sea (KS), Barents Sea (BSS), Greenland Sea (GS), Norwegian Sea (NS), and Baffin Bay (BB). The main rivers around the Arctic region are the Mackenzie River (MR), Pechora (PR), the Ob (OB), Yenisey River (YR), Lena River (LR), and Indigirka River (IR). TP indicates the Taymyr Peninsula.

Moved (insertion) [2]

Formatted: Font: 12 pt, Font colour: Auto

Formatted: Centred

Moved up [1]: ¶

Fig.

Deleted: ¶

Deleted: 1

Formatted: Font: Bold

Deleted: There are

Deleted: noted by the marks

Deleted: <object>¶

Formatted: Font colour: Black

Formatted: Normal, Right: 0.63 cm, Border: Top: (No border), Bottom: (No border), Left: (No border), Right: (No border), Between : (No border), Tab stops: 7,96 cm, Centred + 15,92 cm, Right

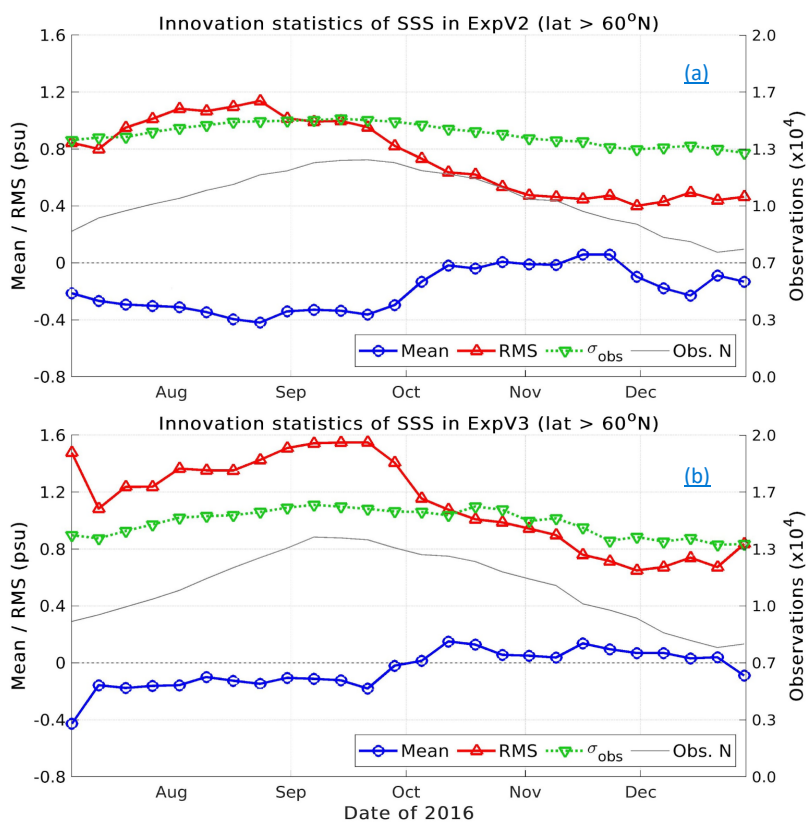


Fig. 3 Innovation statistics of SSS in the Arctic (>60°N) from ExpV2 (a) and ExpV3 (b). The line with red triangles is the root mean squared innovation, and the blue dotted line shows the mean of innovations north of 60°N. The gray line represents the number of observations assimilated, and the green line with inverted triangles is the observation error standard deviation in the two runs.

Deleted: 2. Innovations

Deleted: both weekly assimilation runs

Deleted:

Deleted: ¶
<object>

Formatted: Font colour: Black

Formatted: Normal, Right: 0.63 cm, Border: Top: (No border), Bottom: (No border), Left: (No border), Right: (No border), Between : (No border), Tab stops: 7,96 cm, Centred + 15,92 cm, Right

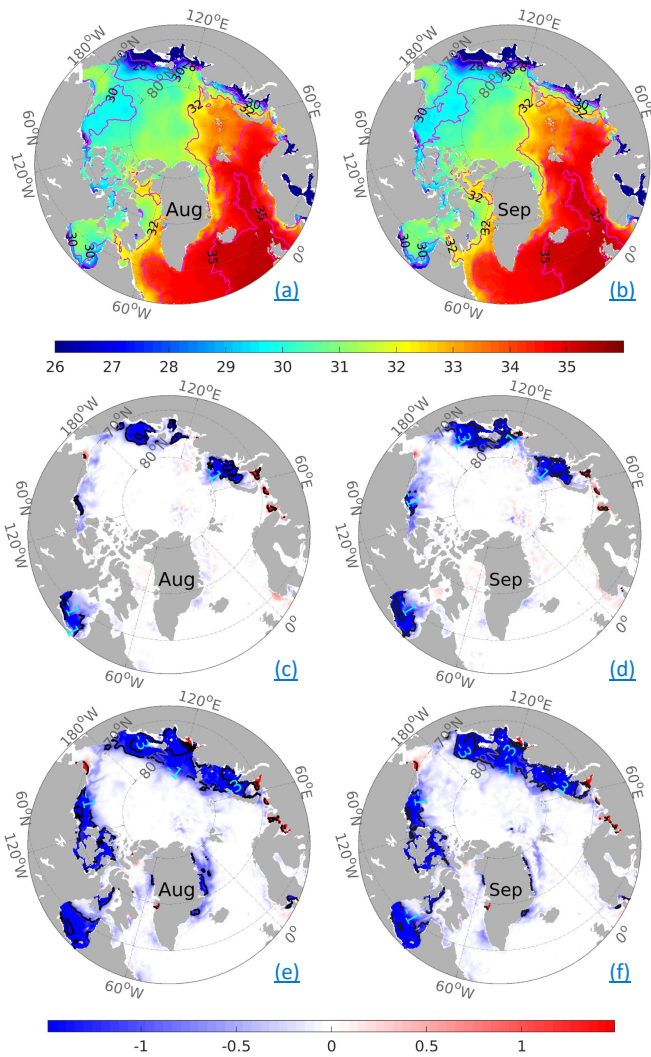


Fig. 4 Top: Monthly simulated SSS (unit: psu) from Exp0 in August (left column) and September 2016 (right column). The black isolines indicate the 26, 28, 30, 32, 34, and 35 psu, respectively. **Middle and bottom:** monthly SSS differences in ExpV2 (middle line) and ExpV3 (bottom line) with respect to Exp0. The black lines are -3, -1, 1, and 3 psu.

Deleted: 3

Deleted: .

Deleted: isolines.

Deleted:

Deleted:),

Deleted:).

Formatted: Font colour: Black

Formatted: Normal, Right: 0.63 cm, Border: Top: (No border), Bottom: (No border), Left: (No border), Right: (No border), Between : (No border), Tab stops: 7,96 cm, Centred + 15,92 cm, Right

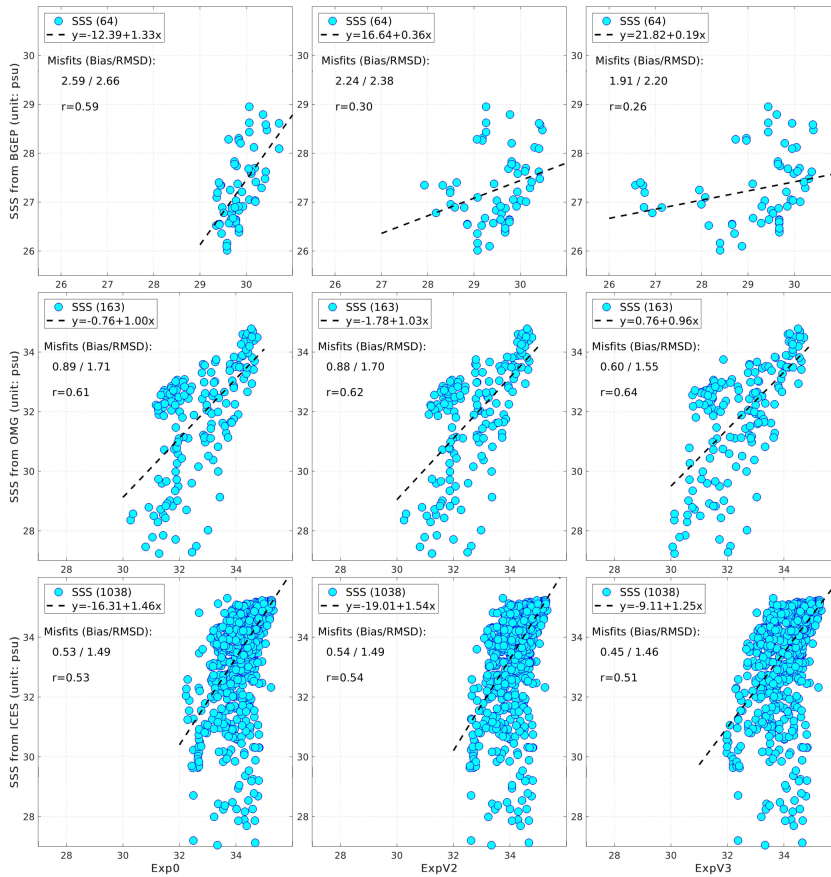


Fig. 5 Scatterplots of SSS in the TOPAZ assimilation runs against in-situ profiles (Top: from BGEF in the Beaufort Sea; Middle: from OMG in both Greenland Seas; Bottom: from ICES in the Nordic Seas as indicated in Fig.1 and descriptions in 2.1). The statistics of SSS misfits are indicated in each panel with the bias and the RMSD, respectively, the number of observations is given between parentheses. The dark dashed line represents the linear regression, and r is the linear correlation coefficient. All the correlation coefficients are over the 95% significance test ($\alpha=0.05$).

Deleted: ¶

<object><object><object>¶

Deleted: 4

Deleted: Upper

Deleted: , and the

Deleted: .

Formatted: Font: 12 pt

Deleted: ¶

<object>¶

Formatted: Font colour: Black

Formatted: Normal, Right: 0.63 cm, Border: Top: (No border), Bottom: (No border), Left: (No border), Right: (No border), Between : (No border), Tab stops: 7,96 cm, Centred + 15,92 cm, Right

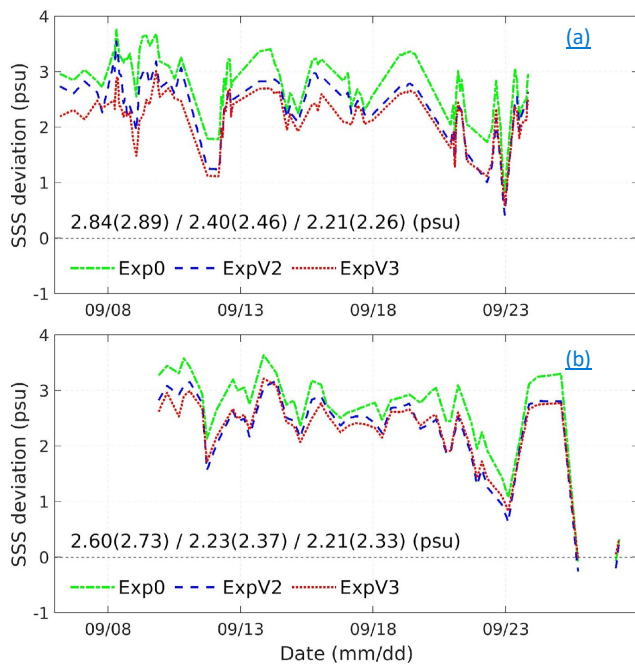


Fig. 6 Model-minus-observations SSS differences in the three assimilation runs against the SSS recorded in the Beaufort Sea and the Chukchi Sea along the SKQ cruise in 2016: a) from CTD profiles; b) from surface water samples underway in the same cruise. The biases are indicated in the same order and the corresponding RMSD [are](#) between parentheses.

Deleted: 5

Formatted: Font colour: Black

Formatted: Normal, Right: 0.63 cm, Border: Top: (No border), Bottom: (No border), Left: (No border), Right: (No border), Between : (No border), Tab stops: 7,96 cm, Centred + 15,92 cm, Right

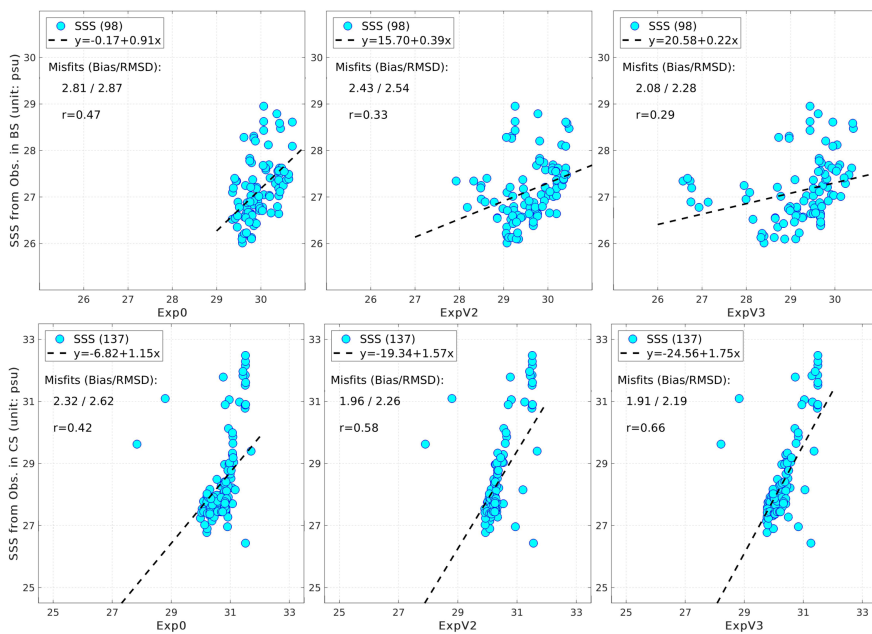


Fig. 7 Scatterplots of SSS (unit: psu) in the three assimilation runs Exp0, ExpV2, and ExpV3 against the CTD observations collected by different cruises in 2016. **Top:** Beaufort Sea; **Bottom:** Chukchi Sea as shown in Fig.1. **All the correlation coefficients are over the 95% significance test ($\alpha=0.01$).**

Deleted: ¶
 ¶
 <object><object>¶

Formatted: Font: 14 pt, Not Bold
 Deleted: 6
 Deleted: of
 Deleted: observations from the
 Deleted: profiles
 Deleted: Upper: in the
 Deleted: in the
 Formatted: Font: 14 pt

Formatted: Font colour: Black
 Formatted: Normal, Right: 0.63 cm, Border: Top: (No border), Bottom: (No border), Left: (No border), Right: (No border), Between : (No border), Tab stops: 7,96 cm, Centred + 15,92 cm, Right

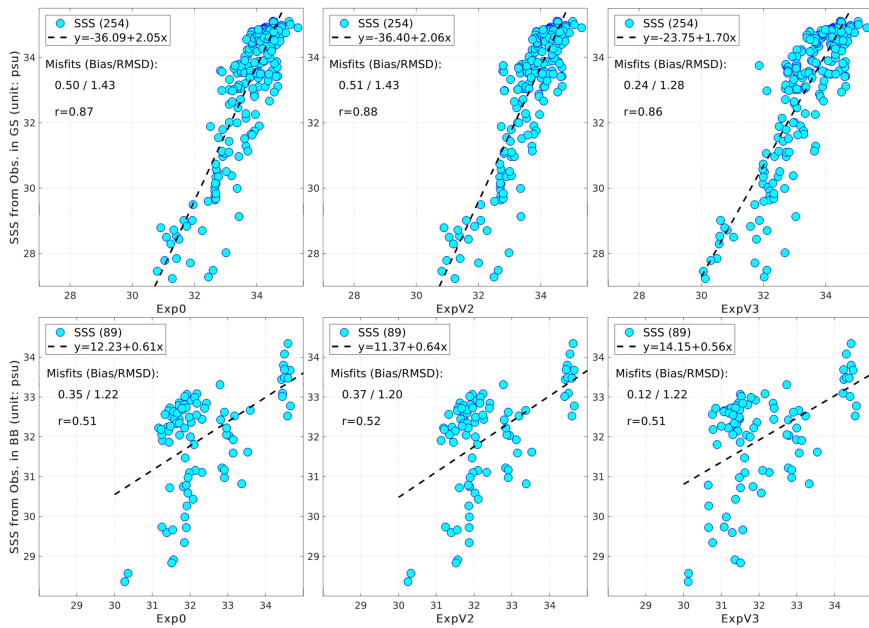


Fig. 8 Scatterplots of SSS (unit: psu) in the three assimilation runs Exp0, ExpV2, and ExpV3 against CTD observations from OMG and ICES in 2016. **Upper:** East Greenland Sea; **Bottom:** Baffin Bay as shown in Fig. 1. The statistics of SSS misfits are indicated in each panel with the bias and the RMSD respectively, and the number of observations is given between parentheses. The dark dashed line represents the linear regression, and r is the linear correlation coefficient. All the correlation coefficients are over the 95% significance test ($\alpha=0.01$).

Deleted: ¶
 Deleted: <object>¶
 Deleted: 7
 Deleted: of
 Deleted: the collected
 Deleted: with the CTD profiles
 Deleted: in the
 Formatted: Font colour: Auto
 Deleted: East
 Deleted: in
 Deleted: <object>
 Formatted: Font: 12 pt

Formatted: Font colour: Black
 Formatted: Normal, Right: 0.63 cm, Border: Top: (No border), Bottom: (No border), Left: (No border), Right: (No border), Between : (No border), Tab stops: 7,96 cm, Centred + 15,92 cm, Right

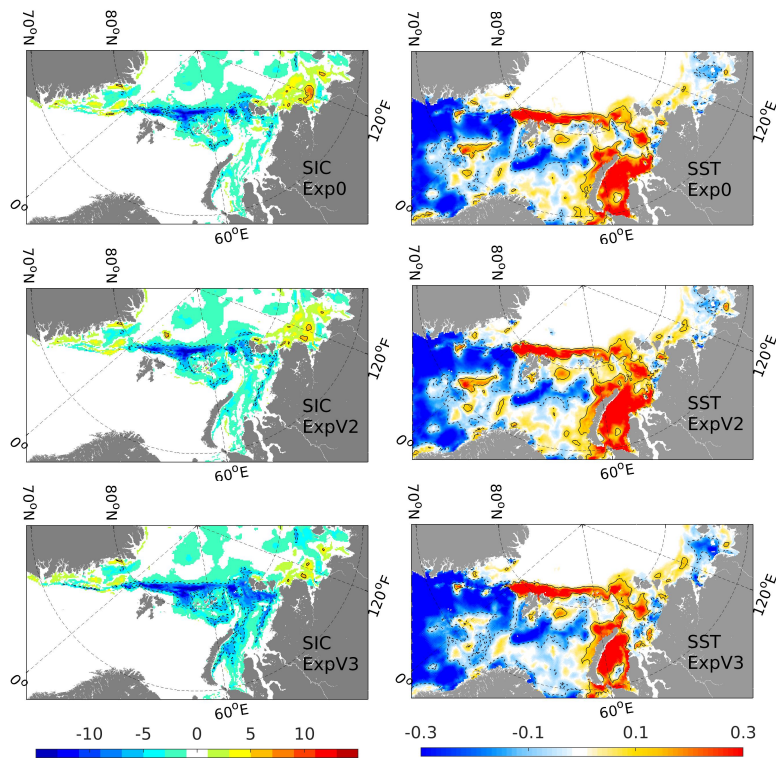


Fig 9. Averaged increments for the 6-months period (Top: in Exp0; Middle: in ExpV2; Bottom: in ExpV3). The figure shows the European Arctic for clarity. Left column: sea ice concentration (unit: %) with isolines of $\pm 5\%$. Right column: SST with isolines of $\pm 0.1^\circ\text{C}$.

Deleted: ¶

¶

¶

¶

¶

¶

¶

¶

¶

¶

¶

<object>¶

¶

¶

¶

Deleted: 8

Deleted: increment of SSS

Deleted: (a),

Deleted: (b) and

Deleted: (c

Deleted: obvious changes of SSS (± 0.1 psu) are highlighted by

Formatted: Font: 12 pt, Font colour: Auto

Deleted: ¶

<object>

Formatted: Font colour: Black

Formatted: Normal, Right: 0.63 cm, Border: Top: (No border), Bottom: (No border), Left: (No border), Right: (No border), Between : (No border), Tab stops: 7.96 cm, Centred + 15.92 cm, Right

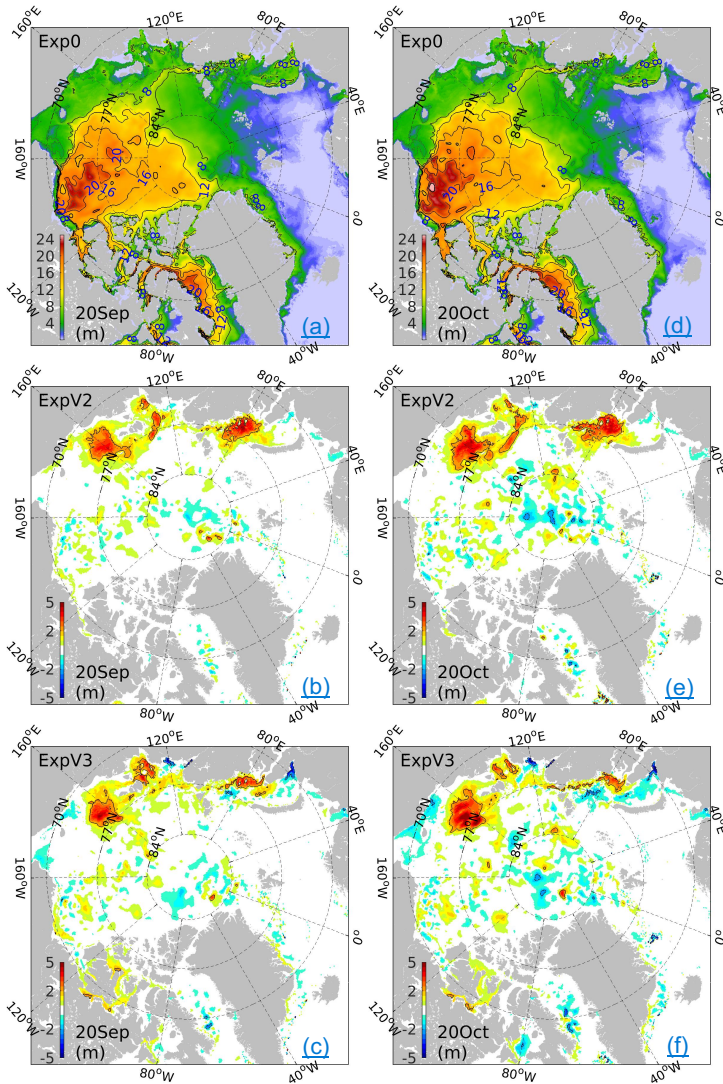


Fig. 10 Top: Freshwater contents (unit: m) on 20th September and 20th October 2016 in the Arctic Ocean from the three assimilation runs: Exp0. The interval of isolines is 4 meters. **Middle and bottom:** the FWC differences in ExpV2 (middle line) and ExpV3 (bottom line) concerning that in Exp0. The black lines indicate -2 m and 2 m differences.

Moved up [2]:

Deleted: 9. Daily freshwater content depths

Formatted: Font: 12 pt, Font colour: Auto

Deleted: (a; d), ExpV2 (b; e), and ExpV3 (c; f).

Formatted: Font colour: Black

Formatted: Normal, Right: 0.63 cm, Border: Top: (No border), Bottom: (No border), Left: (No border), Right: (No border), Between : (No border), Tab stops: 7.96 cm, Centred + 15.92 cm, Right

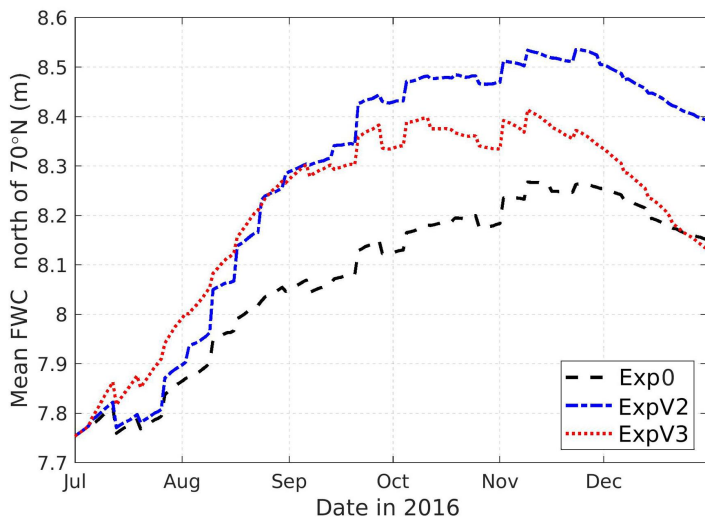


Fig 11. Arctic-wide averaged freshwater content (unit: m) in the central Arctic (>70°N) from July to December 2016 for Exp0 (dark dashed), ExpV2 (blue dashed), and ExpV3 (red dotted).

Deleted: ¶
 ¶
 <object>¶
 ¶

Deleted: 10. Mean
 Deleted: depths
 Deleted: during the period
 Deleted:Section Break (Next Page).....

Formatted: Font colour: Black
 Formatted: Normal, Right: 0.63 cm, Border: Top: (No border), Bottom: (No border), Left: (No border), Right: (No border), Between : (No border), Tab stops: 7,96 cm, Centred + 15,92 cm, Right